NAVAL POSTGRADUATE SCHOOL
Monterey, California

THESIS

HEAT TRANSFER STUDIES AND FLOW VISUALIZATION OF A RECTANGULAR CHANNEL WITH AN OFFSET STRIP FIN ARRAY

by

Ata Komral

September 1995

Thesis Advisor: M. D. Kelleher

Approved for public release; distribution is unlimited.

DISCLAIMER NOTICE

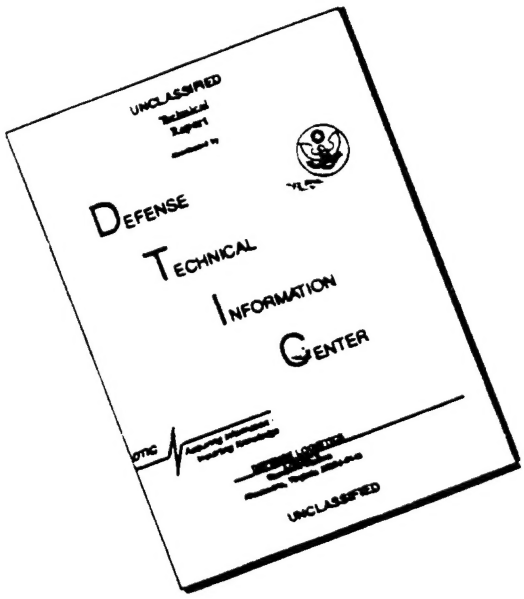

THIS DOCUMENT IS BEST QUALITY AVAILABLE. THE COPY FURNISHED TO DTIC CONTAINED A SIGNIFICANT NUMBER OF PAGES WHICH DO NOT REPRODUCE LEGIBLY.

DISCLAIMER NOTICE

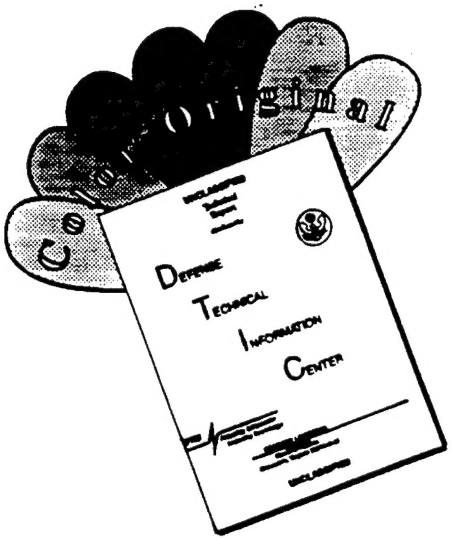

THIS DOCUMENT IS BEST QUALITY AVAILABLE. THE COPY FURNISHED TO DTIC CONTAINED A SIGNIFICANT NUMBER OF COLOR PAGES WHICH DO NOT REPRODUCE LEGIBLY ON BLACK AND WHITE MICROFICHE.

REPORT DOCUMENTATION PAGE

Form Approved OMB No. 0704

1. AGENCY USE ONLY *(Leave blank)*	2. REPORT DATE	3. REPORT TYPE AND DATES COVERED
	September 1995	Master's Thesis

4. TITLE AND SUBTITLE **HEAT TRANSFER STUDIES AND FLOW VISUALIZATION OF A RECTANGULAR CHANNEL WITH AN OFFSET STRIP FIN ARRAY**

5. FUNDING NUMBERS

6. AUTHOR(S) Komral, Ata

7. PERFORMING ORGANIZATION NAME(S) AND ADDRESS(ES)
Naval Postgraduate School
Monterey CA 93943-5000

8. PERFORMING ORGANIZATION REPORT NUMBER

9. SPONSORING/MONITORING AGENCY NAME(S) AND ADDRESS(ES)

10. SPONSORING/MONITORING AGENCY REPORT NUMBER

11. SUPPLEMENTARY NOTES The views expressed in this thesis are those of the author and do not reflect the official policy or position of the Department of Defense or the U.S. Government.

12a. DISTRIBUTION/AVAILABILITY STATEMENT
Approved for public release; distribution unlimited

12b. DISTRIBUTION CODE

13. ABSTRACT *(maximum 200 words)*

In this study, the offset strip fin array in a liquid flow through module was examined. The study used a model of the heat exchanger which is ten times larger than the actual model used in electronics cooling. Water and Brayco Micronic 889 Polyalphaolefin were used as the working fluids in order to determine the Reynolds number and Prandtl number effects on the Colburn j factor. Also, flow visualization experiments were performed to determine the flow characteristics of the offset strip fins for laminar flow.

14. SUBJECT TERMS Offset Strip Fins

15. NUMBER OF PAGES
99

16. PRICE CODE

17. SECURITY CLASSIFICATION OF REPORT	18. SECURITY CLASSIFICATION OF THIS PAGE	19. SECURITY CLASSIFICATION OF ABSTRACT	20. LIMITATION OF ABSTRACT
Unclassified	Unclassified	Unclassified	UL

NSN 7540-01-280-5500

Standard Form 298 (Rev. 2-89)
Prescribed by ANSI Std. 239-18 298-102

Approved for public release; distribution is unlimited.

HEAT TRANSFER STUDIES AND FLOW VISUALIZATION OF A RECTANGULAR CHANNEL WITH AN OFFSET STRIP FIN ARRAY

Ata Komral
Lieutenant Junior Grade, Turkish Navy
B.S., Turkish Naval Academy, 1989

Submitted in partial fulfillment
of the requirements for the degree of

MASTER OF SCIENCE IN MECHANICAL ENGINEERING

from the

NAVAL POSTGRADUATE SCHOOL
September 1995

Author: _____
Ata Komral

Approved by: _____
Matthew D. Kelleher, Thesis Advisor

_____
Matthew D. Kelleher, Chairman
Department of Mechanical Engineering

ABSTRACT

In this study, the offset strip fin array in a liquid flow through module was examined. The study used a model of the heat exchanger which is ten times larger than the actual model used in electronics cooling. Water and Brayco Micronic 889 Polyalphaolefin were used as the working fluids in order to determine the Reynolds number and Prandtl number effects on the Colburn j factor. Also, flow visualization experiments were performed to determine the flow characteristics of the offset strip fins for laminar flow.

TABLE OF CONTENTS

LIST OF FIGURES

LIST OF TABLES

ACKNOWLEDGMENT

I would like to express my sincere appreciation to those who kept me going through of this thesis .

Professor Kelleher, who always provided me with help, advise, and constructive commentary.

My Friend Erkan Yeniceri, who took time from his studies to take photographs during the flow visualization experiments.

Jennifer Campbell, who has been a great companion and a continuous source of support and motivation.

Jim Scholfield, who always found time to help about technical matters.

I. INTRODUCTION

A. ELECTRONIC COOLING

The trend in electronic packaging has been towards building more electronic circuits into one very small chip. Since the invention of the silicon integrated circuit, there has been an increase in the number of components per chip. This increase in circuit integration continues to be driven by the need for increased processing speed. With each increase in the scale of integration of microelectronic circuits more effective cooling systems are required.

Currently, chip heat fluxes are approaching 50 W/cm^2 and heat fluxes of 200 W/cm^2 are projected [Ref. 1]. Also, it is known that chip temperatures must be maintained within prescribed operating limits below 85° C. Due to the large heat fluxes and small areas associated with current and projected very large scale integrated circuits and the maximum allowable junction temperature requirement, it could be necessary to cool the system by liquid cooling and to enhance heat transfer by using extended surfaces.

B. LIQUID COOLING METHOD

At lower air velocities, typical heat flux limits for packages cooled by conventional forced convection are less than 1 W/cm^2 [Ref. 2]. Because of the high heat fluxes of today's technology, it is evident that air cooling could not provide an optimal solution to the cooling problem. As a result of the higher density and thermal conductivity of liquids in comparison to air, it is possible to enhance heat transfer coefficients by using liquid cooling.

1. Direct Liquid Cooling

Direct liquid cooling maintains physical contact between the coolant and the electronic components. The coolant should have dielectric characteristics and good chemical compatibility so as not to effect the circuit performance.

2. Indirect Liquid Cooling

Indirect liquid cooling cools the electronic components with attachment of a liquid cooled plate/heat exchanger to the electronic package (See Figure 1). This cooling technique requires the addition of a liquid circulating pump. The significant advantage of this cooling method is the reduction in the thermal resistance to heat transfer.

Modules are usually enclosed in protective covers to which fins may be attached to enhance heat transfer to an external coolant.

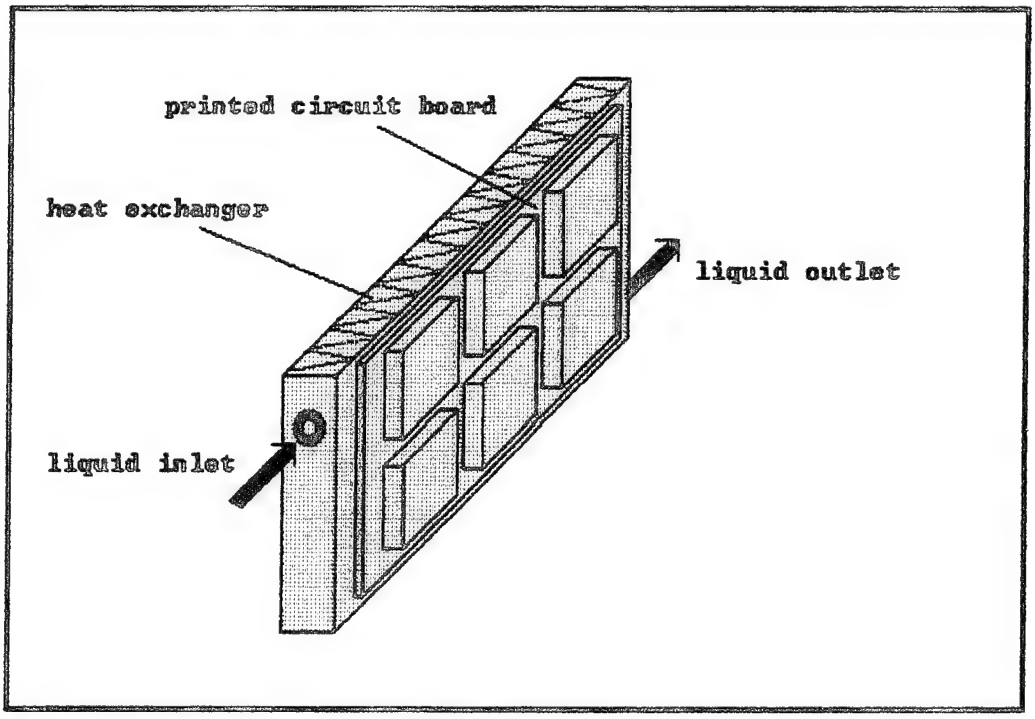

Figure 1. Liquid Cooled Integral Heat Exchanger.

C. OFFSET STRIP FINS

1. Characteristics of Offset Strip Fins

Offset strip fin is one of the most widely used fin geometries in compact heat exchangers. The cross section of the fin is rectangular. The fin is cut into small strips of length *l* in the flow direction. The other variables are the fin spacing s, fin height h, and fin thickness t. The offset is about 50 % of the fin pitch (See Figure 2).

The offset strip fins have high heat transfer coefficients. This is mainly caused by the developing laminar boundary layers. The interrupted geometry of the fins prevents the velocity and temperature boundary layers from getting excessively thick. Since the form drag increases due to the finite thickness of the fins the friction factors are also high. In this study the offset strip fin array in a liquid flow through module (LFM) used in electronics cooling is examined. The study uses a model of the heat exchanger which is ten times larger than the actual model. A typical liquid flow through module is shown in Figure 3.

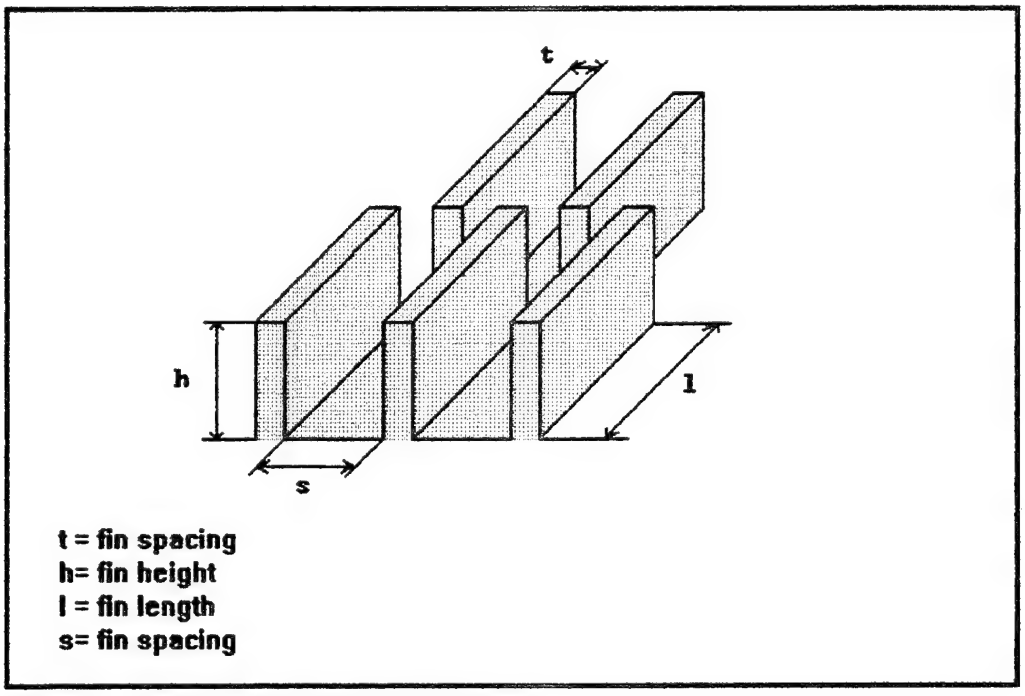

Figure 2. Typical Offset Strip Fin Geometry.

2. Analytical and Numerical Correlations for Offset Strip Fins

Weiting [Ref. 3] correlated available experimental heat transfer and flow friction data for 22 offset strip fin surfaces using air as the working fluid. Weiting defines the Reynolds number based on the hydraulic diameter as follows;

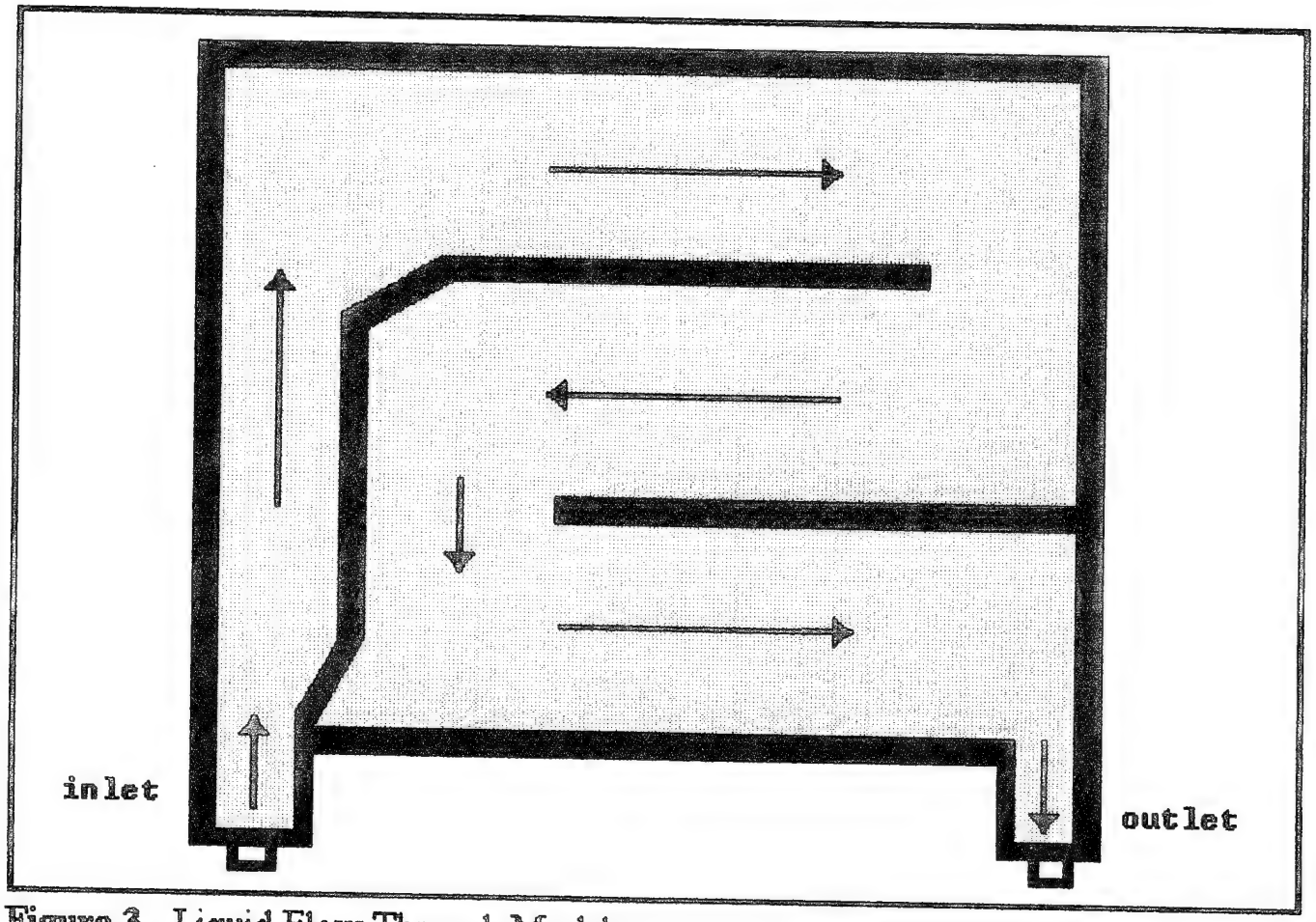

Figure 3. Liquid Flow Through Module.

$$Re = \frac{U \times D_h}{\nu} \qquad \text{Equation 1.1}$$

Here U is the mean velocity of the air in the channel, ν is the kinematic viscosity of the air and D_h is the hydraulic diameter ($D_h = 4A_c/P$) where A_c represents the cross-sectional area and P represents the perimeter of the channel. Weiting's correlations were as follows;

For $Re_D \leq 1000$,

$$f = 7.661(l/D_h)^{-0.384}(\alpha^*)^{-0.092}Re_D^{-0.712} \qquad \text{Equation 1.2}$$

$$j = 0.483(l/D_h)^{-0.162}(\alpha^*)^{-0.184}Re_D^{-0.536} \qquad \text{Equation 1.3}$$

For $Re_D \geq 2000$,

$$f = 1.136(l/D_h)^{-0.781}(\delta/D_h)^{0.534}Re_D^{-0.198} \qquad \text{Equation 1.4}$$

$$j = 0.242(l/D_h)^{-0.322}(\delta/D_h)^{0.089}Re_D^{-0.368} \qquad \text{Equation 1.5}$$

Here l is the strip length, δ is the fin thickness, D_h is the hydraulic diameter of the passages and α^* is the ratio of the width to height of the passage. For Reynolds numbers in the laminar range he stated that the Colburn j factor was only a function of Reynolds number and l/D_h or α^*. He considered the correlation to be accurate within $\pm$ 10 %, though some points deviated by forty percent.

Manglik and Bergles [Ref. 4], gathered all the previously taken data for the offset strip fins and developed a correlation for the Colburn j factor which can be used for both the laminar and turbulent regions. Their definition of Reynolds number and hydraulic diameter was the same with Weiting's definition.

$$j = 0.6522(s/h)^{-0.1541}(t/l)^{0.1499}(t/s)^{-0.0678}Re_D^{-05403} \qquad \text{Equation 1.6}$$

In their correlation, s is the fin spacing, h is the fin height, t is the fin thickness and l is the fin length. They state that this correlation is applicable for Prandtl numbers in the range of 0.5 to 15. They estimated their correlation to be accurate within ± 20 %.

The correlations for the transition from laminar to turbulent region were developed by H. M. Joshi and R. Webb [Ref. 5]. They used a numerical solution for the Nusselt number and the friction factor for a laminar flow and a semi-emprical solution for the turbulent region.

For $Re_D \leq 1000$,

$$j = 0.53(l/D_h)^{-0.15}(s/h)^{-0.02}Re_D^{-0.50} \qquad \text{Equation 1.7}$$

For $Re_D \geq Re_D + 1000$,

$$j = 0.21(l/D_h)^{-0.24}(t/D_h)^{0.02}Re^{-0.40} \qquad \text{Equation 1.8}$$

Several attempts have been made to predict analytically the heat transfer and flow friction characteristics of offset strip fins. One of the first attempts was made by Kays [Ref. 6]. He used Pohlhausen laminar boundary layer solution for a flat plate to calculate the heat transfer from an offset strip fin. For friction, he used the Blasius laminar boundary layer solution for a flat plate. His Reynolds number was not based on the hydraulic diameter but on the length of the flat plate ($Re_l = U \cdot l/\nu$). His results were as follows;

$$j = 0.664Re_l^{-0.5} \qquad \text{Equation 1.9}$$

$$f = \frac{C_D^{\delta}}{2^l} + 1.328Re_l^{-0.5} \qquad \text{Equation 1.10}$$

Here l is the fin length, δ is the fin thickness and C_D is the drag coefficient. Kays suggested C_D=0.88 based on the potential flow normal to a flat plate. In this model

it is idealized that the velocity and temperature boundary layers are destroyed in the wake region. Although this model is at best a first order approximation, it does not provide the detailed insight into the systems . Patankar and Prakash [Ref. 7], predicted the j and f factors for the offset strip fins numerically by a finite difference method. They considered the laminar boundary layers on each strip fin. They first assumed that strip fins have infinite height and zero thickness. Then they extended the analysis for finite fin thickness. They observed that at low Reynolds Numbers or low δ/s, the recirculation zone behind the trailing edge was small. At high Reynolds numbers or high δ/s, this recirculation zone extended from the trailing edge to the next strip. (See Figure 4).

Although a large amount of experimentation and numerical predictions have been made, further studies and improvements are needed to accurately understand the performance of the offset-strip fins.

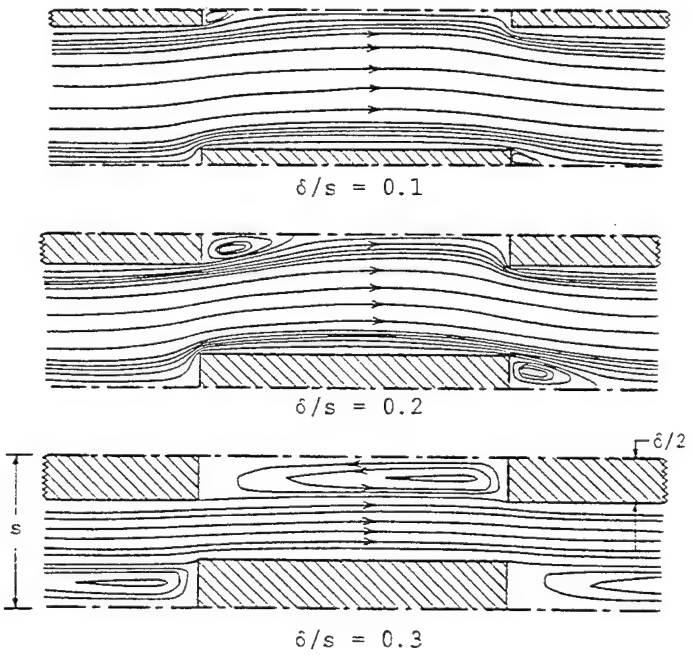

Figure 4. Flow Patterns Over Offset Strip Fins At Different δ/s for Re_D=2000, Based On A Numerical Solution, From Ref. 7.

D. OBJECTIVES OF PRESENT STUDY

The first objective of this study was to investigate the heat transfer characteristics of a liquid flow through module which is actually a ten times scaled up model of the fluid circulation passages of an SEM-E (Liquid Flow Through Module). By using water and Brayco Micronic 889 (Castrol) Polyalphaolefin (PAO) as the working fluid, experiments were performed to determine the Reynolds number and Prandtl number effects on the dimensionless heat transfer coefficients.

The second objective was to visualize the flow over the offset strip fins which were used to enhance the heat transfer. Dye injection was applied to observe the variation in the velocity boundary layer across the fins and the recirculation of the flow behind the trailing edge of the fins for varying flow rate of the coolant.

II. EXPERIMENTAL APPARATUS

The experimental apparatus included a system to circulate the coolant through the test section and another system to collect the necessary data to be able to calculate the heat transfer and flow characteristics of the test section.

A. COOLANT CIRCULATING SYSTEM

A schematic of the coolant circulation system is shown in Figure 5.

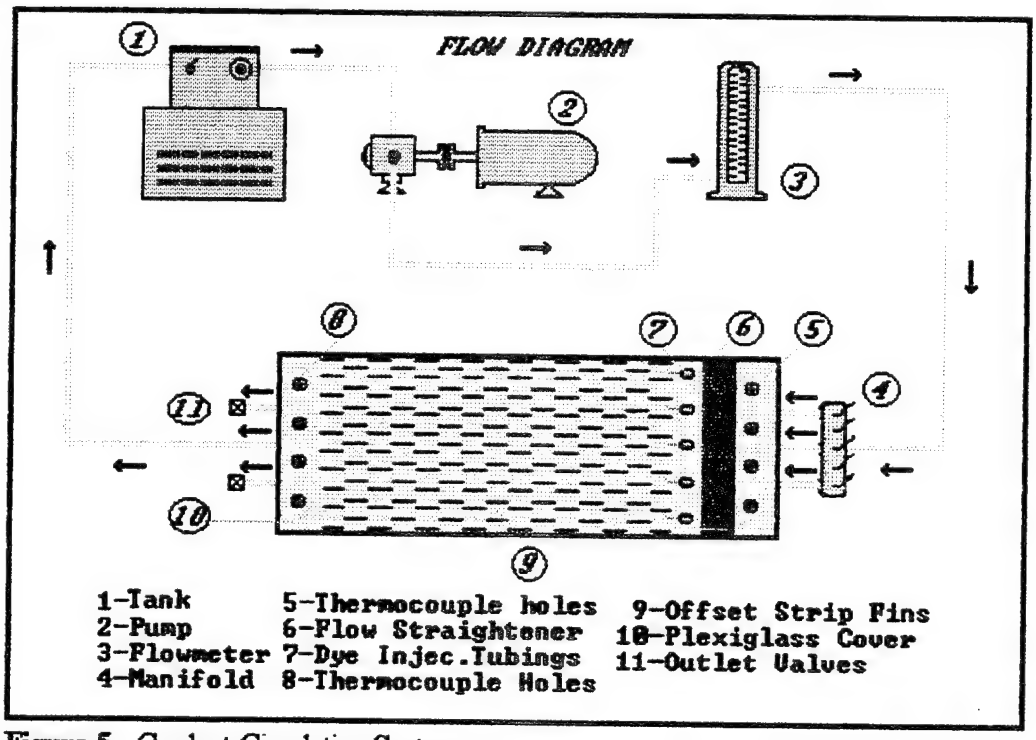

Figure 5. Coolant Circulating System.

1. Liquid Tank

In this study first water and then Brayco Micronic 889 (Castrol) Polyalphaolefin (PAO) were used as the working fluids. In both case, the coolant was provided by an

Endocal RTE-5 circulating bath. The Endocal RTE-5 has a heater/refrigeration unit which enables the regulation of the temperature of the liquid in the bath between -30 to 100 °C. During the experiments this temperature was maintained constant at around 20°C. Since the volume of the circulating bath was small, it was noted that as the Reynolds number exceeded about 650 for water and 60 for Brayco Micronic 889 Polyalphaolefin, the temperature of the liquid in the bath was effected by the hotter liquid at the exit of the heat exchanger which was circulated back to the tank.

2. Pump

A Cole Parmer positive displacement gear type pump was used to circulate the coolant through the heat exchanger. The positive pressure fluid surge volume to the pump was provided by the heater/refrigeration unit of the liquid bath.

The pump was driven by a DC motor. The speed control unit of the DC motor provided varying flow rates and Reynolds numbers for varying pump speeds. For the heat transfer experiments the pump speed was varied between 10-70 % of its maximum value which corresponded to the Reynolds numbers in the range of 50-650 for water and the Reynolds numbers in the range of 10-80 for Brayco Micronic 889 Polyalphaolefin.

It was noted that for small pump speeds the time required by the test section to reach its steady state condition was around 60 minutes. The time required to reach the steady state condition was decreasing with increasing pump speed (increasing Reynolds number).

3. Flowmeter

Following the pump, coolant was passed through an Omega FTB-102 turbine flowmeter to measure the flow rate. As the flow rate varied the voltage across the AC to DC signal converter which was connected to the flowmeter also changed. These voltage outputs were than used to calibrate the flowmeter.

The flowmeter was calibrated for both of the coolants. The calibration of the flowmeter for water was made in two different ways. The first one consisted of a comparison of the average voltage output to the average time to collect a specific volume of water. The second method was based on the collected mass of the water in a specific time for varying pump speeds. Even though the second method produced a more linear calibration curve than the first one, the flow rate measurements, especially in the range of middle Reynolds numbers (200-600), were very close to each other. The calibration of the flowmeter for the PAO was based on the first method. All flowmeter calibration curves were presented as Appendix A.

4. Heat Exchanger

The flowmeter outlet was connected to a manifold and divided into three flow paths before entering the offset strip fin heat exchanger.

a. Offset Strip Fins

The test section which includes the base plate and the offset strip fin assembly was first constructed by Lt. Jeffrey Masterson [Ref. 8]. A picture of the test section is shown in Figure 6. The fin assembly was a 10 times scaled up model of the horizontal passages of a liquid flow through module used in electronics cooling. The base plate consisted of three parts. (The inlet plenum, outlet plenum and the middle part with fins). The inlet and outlet plenum were made from two pieces of a 12.7 mm aluminum 6061 alloy plate. They were milled down to the base plate thickness of 10.16 mm. The middle part of the base plate, which included the offset strip fins, was also made from aluminum 6061 alloy. Instead of welding the fins onto the base plate, the base and the fins were milled from a solid piece, not to leave weld deposits and affect the fin geometry. A 2.54 cm thick aluminum plate was cut into 31.75 mm wide strips. These strips were then milled to the width of the plate. The fins were cut 15.24 mm deep into the aluminum and 15 rows were obtained. Each row had 19 fins where the spacing

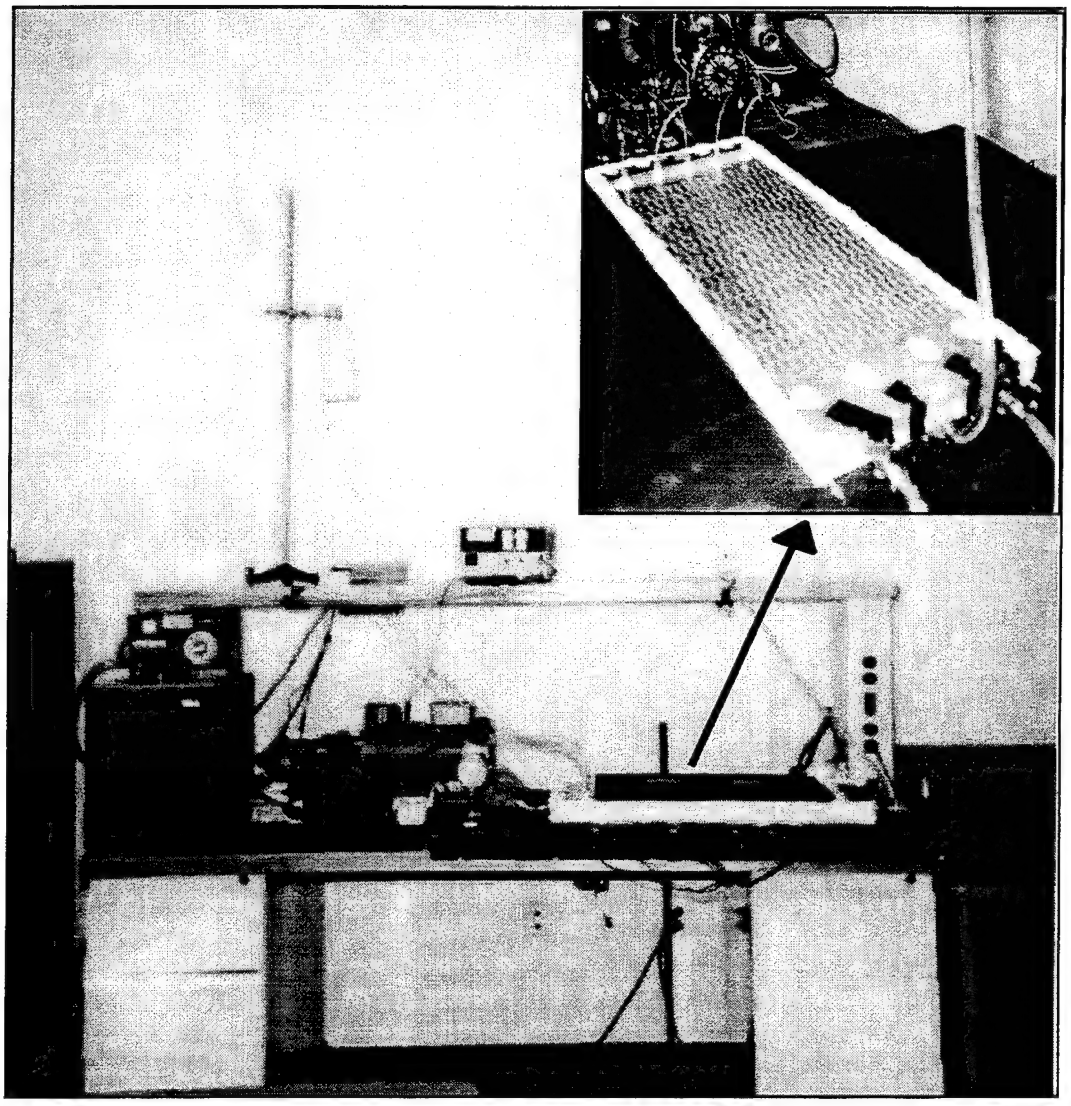

Figure 6. Test Section.

between the fins was 11.76 mm. A 6.64 mm offset was allowed on one end that when alternated created the offset pattern of succeeding fin rows. On each end of the base plate an additional 12.7 mm offset of base plate thickness was milled to attach the plexiglas cover [Ref. 8]. A schematic of the finned section is shown in Figure 7.

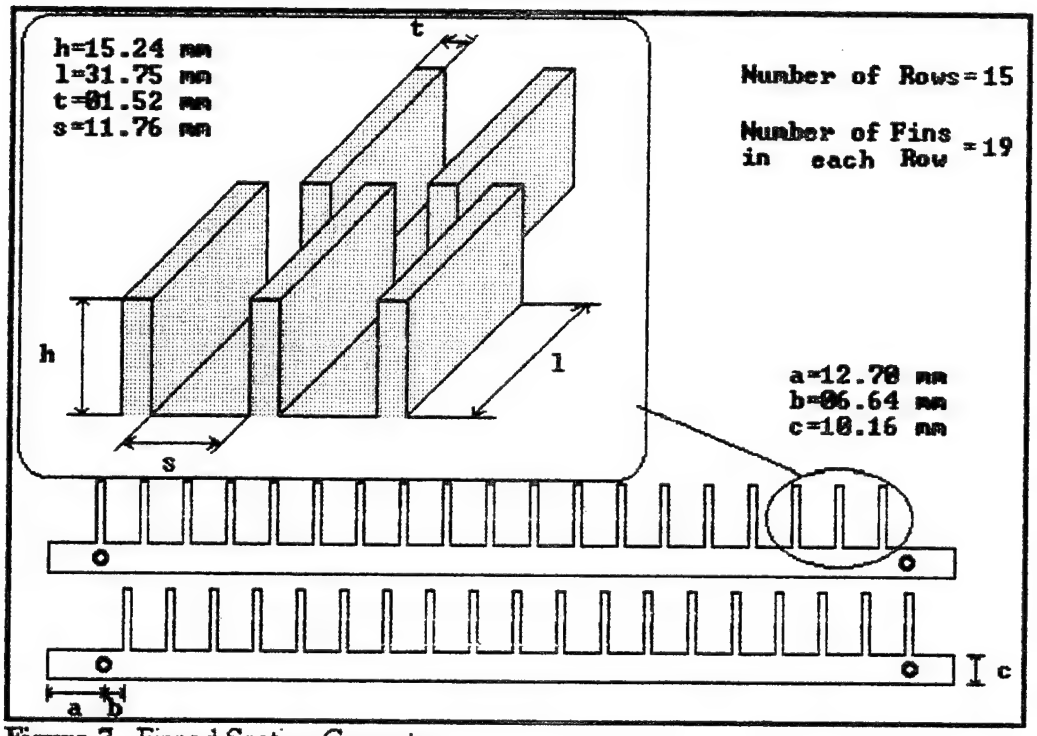

Figure 7. Finned Section Geometry.

The inlet plenum, finned section and the outlet plenum were connected to each other by means of two threaded rods. The holes to accommodate the threaded rods were drilled in the lengthwise direction through each fin row and plenum piece. Rubber gasket was placed between the first row and the inlet plenum sections and between the last row and the outlet plenum sections to reduce the longitudinal conduction losses from the finned section to the plenum. The final assembly was held and tightened by using nuts at each end of the rods [Ref. 8].

The overall dimensions of the test section are shown in Figure 8.

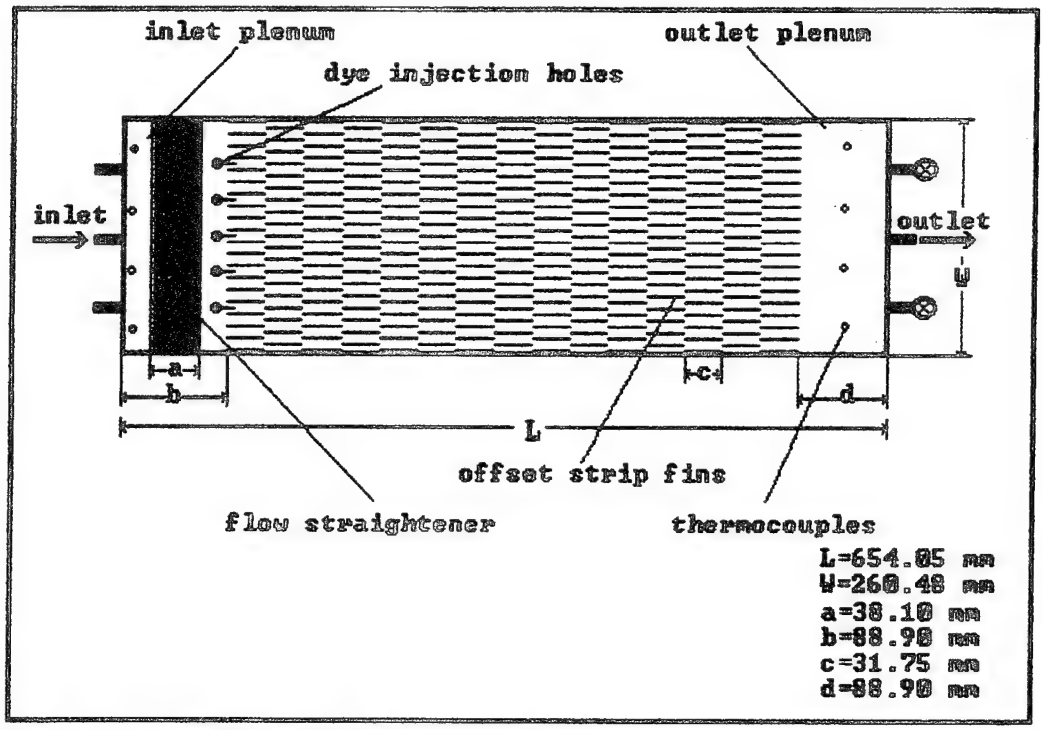

Figure 8. Overall Dimensions of The Test Section.

Since the water left some deposits on the base plate and offset strip fins, the test section was cleaned and sandblasted and prepared for the present study.

b. Plexiglas Cover

The construction of the heat exchanger was completed by enclosing the base plate and fin assembly by a plexiglas cover. Since the original plexiglas cover was deformed a new one was fabricated. The top was cut to the dimensions of the base plate (654x260.5 mm) and the sides were cut to the height of the fins (15.24 mm).

Before attaching the plexiglas cover to the base, all the necessary holes were drilled into the plexiglas cover. Three inlets and three outlets were drilled into the

axial ends of the plexiglas cover. Inlets and outlets consisted of 3.175 mm pipe threads drilled and tapped into the plexiglas wall with 6.35 mm tygon adaptors on the opposite end of the wall. One inlet and one outlet were aligned on the longitudinal axis of the test plate. The two other inlets and outlets were placed 37.9 mm from the outer edges of the plate. Valves were placed on the two other outlets so they could be closed when operating the test section as needed or opened to drain the system after each experiment. During the first runs these outlets with valves were kept closed and the inlet to the circulating bath was provided by only one outlet of the heat exchanger. But since the pressure in the heat exchanger was high especially for $Re > 500$, one of the outlet valves was also kept open which provided the inlet to the circulating bath from two flow paths. This decreased the high back pressure in the heat exchanger.

Another step before attaching the cover to the base plate was to drill the dye injection and temperature probe points into the plexiglas cover. The details about the dye injection points will be given in the next section.

Four temperature probe holes were placed above both the inlet and outlet plenum regions to measure the inlet and outlet temperatures of the coolant. These holes were very tiny and filled with silicone before feeding the thermocouples through the holes.

Prior to attaching the cover to the base a flow straightener was also fixed between the inlet temperature probe and dye injection holes. The original flow straightener which was devised using 38.1 mm long straws and a plastic mesh was glued to the plexiglas cover. The purpose was to provide a uniform flow velocity profile before the first fin row. The distance between the first fin row and the edge of the flow straightener was about 28 mm. After drilling all the necessary holes and fixing the flow straightener, the sides were attached to the top piece using acrylic cement and secured with screws. During the first runs leakage was noted from the temperature probe holes and the side walls of the plexiglas cover. Silicone was run along the sides and refilled into the temperature probe holes. When the heat transfer experiments were completed a

crack was noted on the top piece of the plexiglas cover. Acrylic cement was syringed into the crack to fill the gaps.

The heat exchanger was the last element of the coolant circulating system. The outlet of the heat exchanger was connected to the refrigerated bath and the circulation of the coolant was completed. Flexible Tygon tubing was used to connect the inlet and outlet parts of the coolant circulating system. Clamps were affixed to tighten the connections.

B. DYE INJECTION SYSTEM

A schematic of the dye injection system is shown in Figure 9.

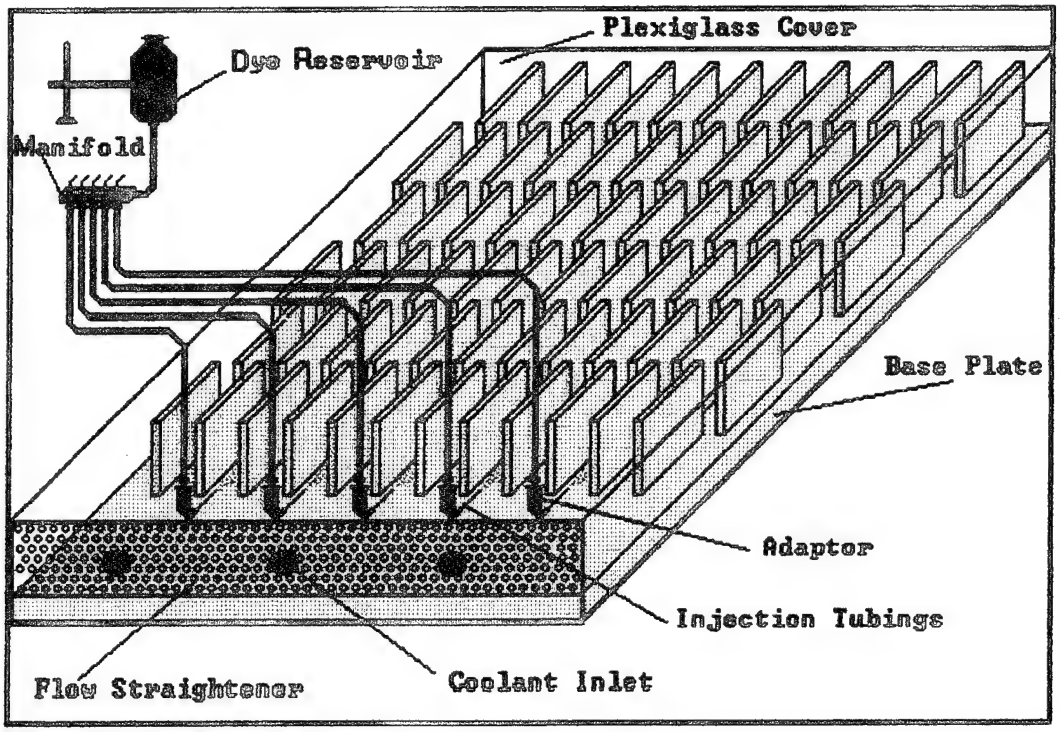

Figure 9. Dye Injection System.

Five dye injection points were placed in the plexiglas cover. They were 1.6 mm holes that penetrated the plexiglas cover just before the first row fins and after flow straightener assembly. Five adaptors were placed into these holes. Inside the plexiglas cover, stainless steel surgical tubing was passed through the adaptors. This tubing was bent into a 90 degree bend and the ends were smoothed and shaped to a cone in order to direct the dye flow between the fins. The total length of a steel tubing was about 50 mm. The other ends of the adaptors which were left on the outside of the plexiglas cover were connected to a manifold by using 190 mm long plastic tubes. The manifold was used to distribute the dye in the reservoir to the desired injection tubings. The reservoir was a small plastic bottle and was held about 1 meter above the test section to provide a positive pressure. A small syringe also served as an ink reservoir.

C. DATA COLLECTING SYSTEM

A heater was used to heat the test section and the temperatures were measured by means of thermocouples. Thermocouples were connected to a data acquisition system which also measured the required voltages. Flow visualization data was recorded by using a 35 mm camera.

1. Heater

Printed circuit boards usually dissipate constant heat flux. This was simulated by using an electrical heater which was a Minco foil backed patch. The heater pad was 25.4 cm by 30.48 cm, resulting in a heater surface area of 774.2 cm^2 .

The heater pad was fixed to the bottom of the aluminum plate with pressure sensitive adhesive. The pad covered the finned area section except 3.24 mm on the sides and 9.525 mm at each end. A Kepco 0-100 V, 0-5 A power supply provided DC power to the heater. A 250 Watt, 2±0.01 Ω precision resistor was connected in series with the heater. The purpose of the precision resistor was to determine the power to the heater.

A schematic of the power distribution system is given in Figure 10. The bottom of the base plate was mounted on foam rubber insulation. The sides and the top surface of the plexiglas cover were also covered with insulation to reduce the heat losses to ambient.

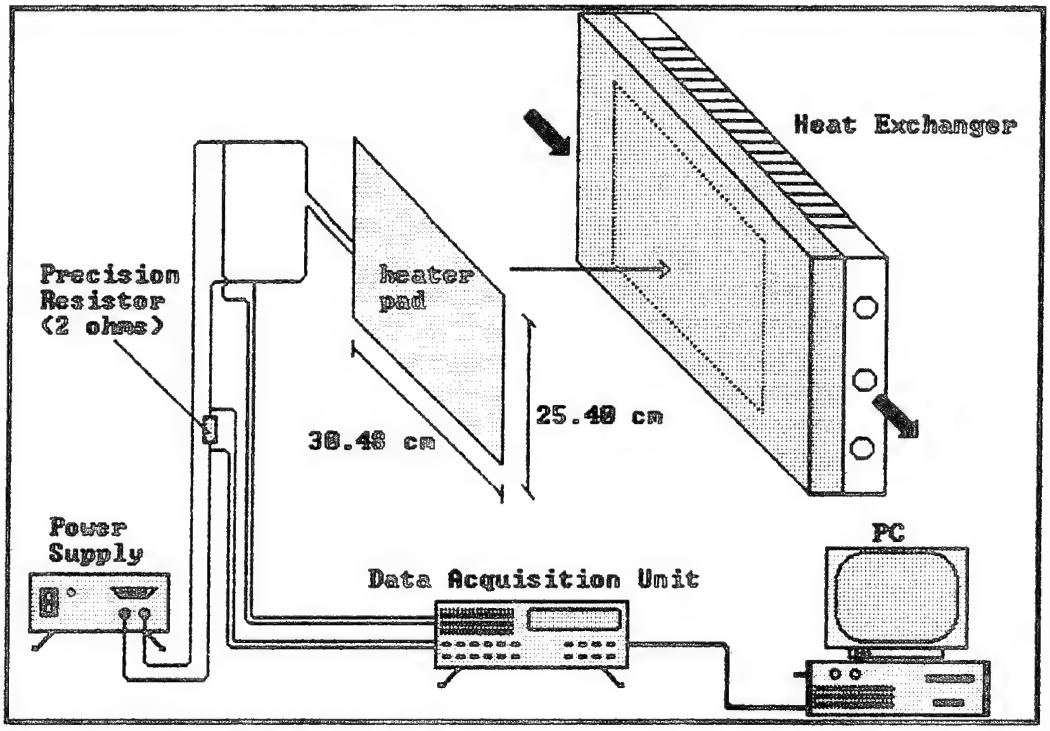

Figure 10. Power Distribution System.

The voltage drops across the precicision resistor and the heater were measured by the Data Acquisition/Control Unit. Since the heater and the precision resistor were connected in series the electrical current passing through the resistor was equal to the current through the heater. The power to the heater was determined using the following relationships, where V_h , was the measured DC voltage across the heater and V_p , the voltage drop across the precision resistor with resistance R.

$$I_p = \frac{V_p}{R} \qquad \text{Equation 2.1}$$

$$I_h = I_p \qquad \text{Equation 2.2}$$

$$Power = I_h \times V_h \qquad \text{Equation 2.3}$$

2. Thermocouples

The temperature of the aluminum base plate was measured by using 23 Copper Constantan (T-Type) cement-on thermocouples. They were placed on the bottom surface of the finned base plate as seen in Figure 11. Since the thermocouples were placed between the heater pad and the base plate, flat ribbon thermocouples were chosen to provide better surface contact. The thermocouples were glued using Omegabond 101 which was a high thermal conductivity epoxy.

Eight Copper Constantan (T-Type) thermocouples were fed through the holes drilled into the plexiglas cover to measure the inlet and outlet coolant temperatures. Two thermocouples were affixed between the plexiglas cover and the insulation layer where the two others were mounted on top of the insulation layer to be able to estimate the heat losses through the cover and the insulation.

Another Copper Constantan (T-Type) thermocouple was placed into the refrigerated bath to measure the coolant temperature in the bath. All the thermocouples were then connected to the Data Acquisition System.

3. Data Acquisition System

All the thermocouples and voltages were measured by an Hewlett Packard 3852 Data Acquisition/Control Unit. Two 24-channel, thermocouple compensated high speed multiplexed boards (HP 44713 A) measured a total number of 34 thermocouple junction temperatures and a 24-channel high speed multiplexed board (HP 44705 A) measured the voltage drops across the flowmeter, precision resistor and the power supply.

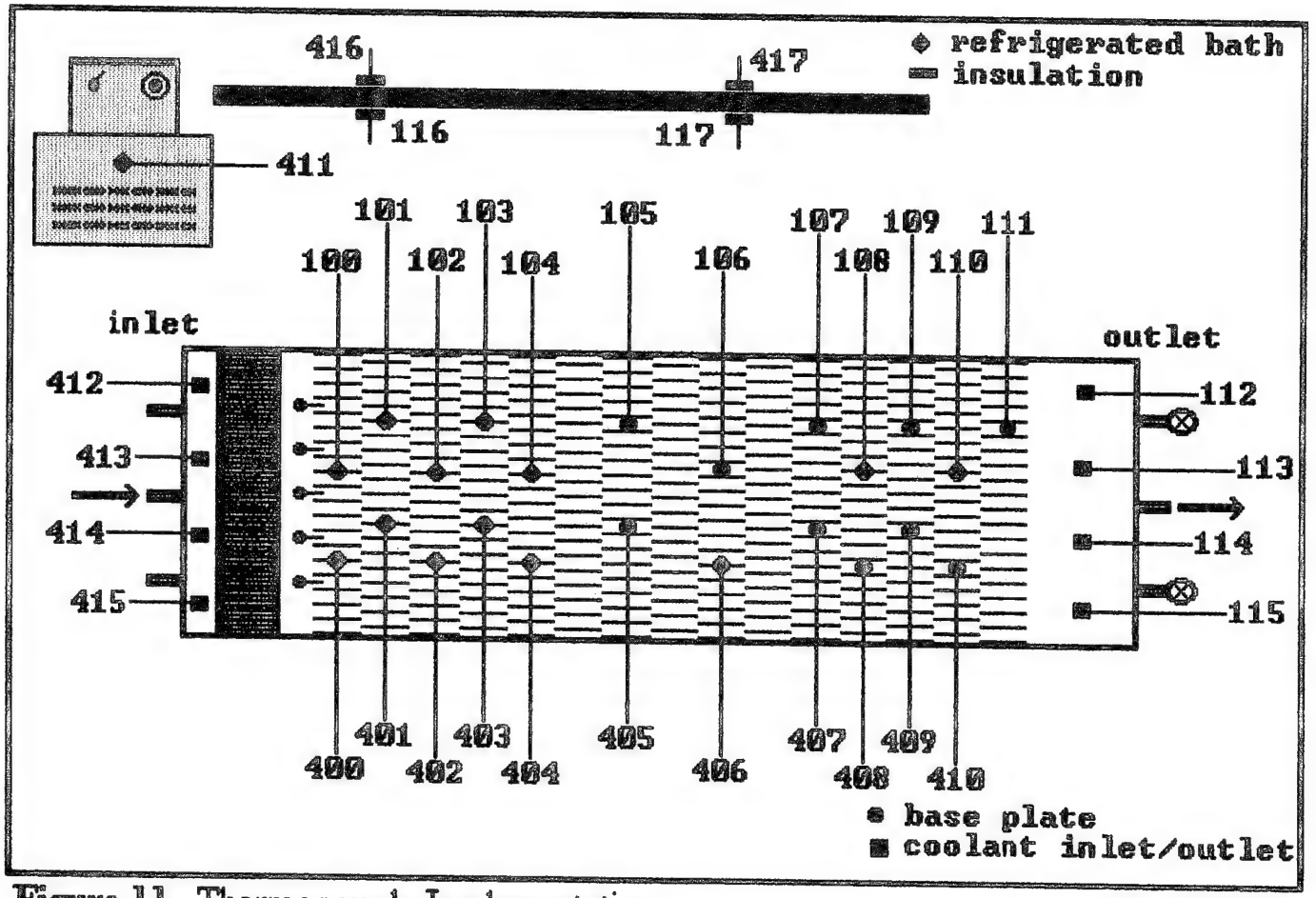

Figure 11. Thermocouple Implementation.

All thermocouple extensions were labeled and plugged into channel numbers 0 through 17 of both HP 44713 A boards and the voltage drops were measured by the channels 0 through 2 of the HP 44705 A board.

The Data Acquisition Unit was controlled by a Personal Computer. An interface board, G PIB-PCIIA IEEE-488, manufactured by National Instruments was installed into this computer. A program attached as Appendix B was written in QBASIC code to store the data for later computation and display. A schematic of the entire experimental apparatus is presented in Figure 12.

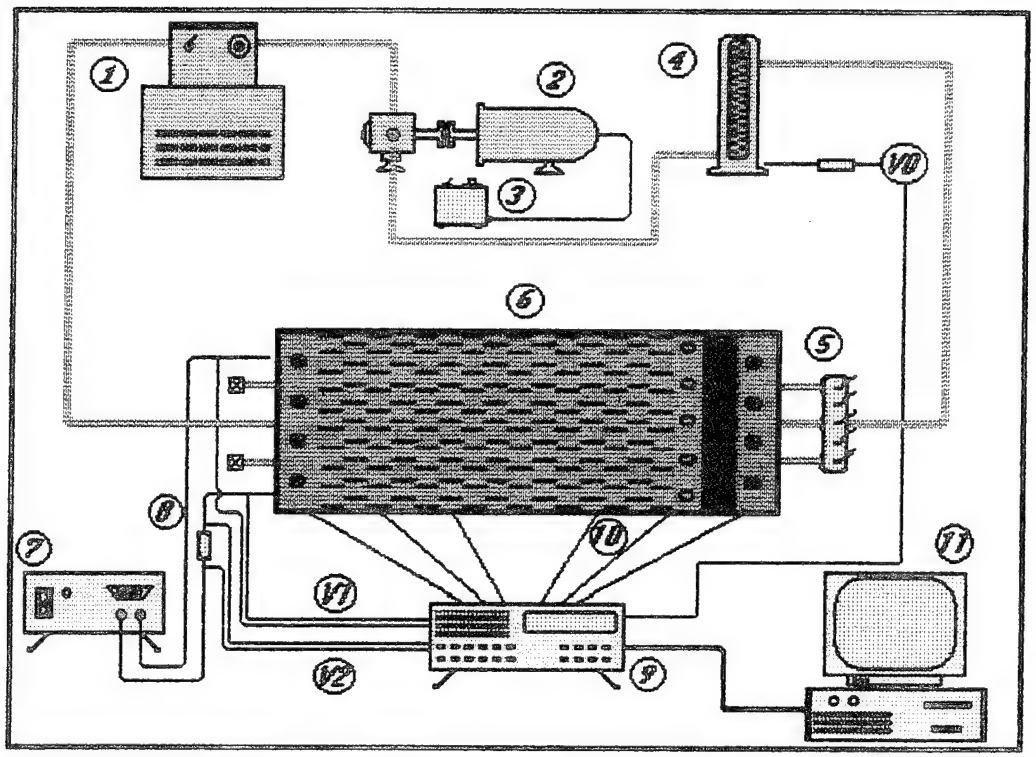

Figure 12. The Entire Experimental Apparatus.

1- Refrigerated Tank
2- Pump
3- Pump Speed Control
4- Flowmeter
5- Manifold
6- Heat Exchanger
7- Power Supply
8- Precision Resistor
9- Data Acquisition Unit
10- Thermocouples
11- Personel Computer
V0- Voltage (Flowmeter)
V1- Voltage (Heater)
V2- Voltage (P.resistor)

III. EXPERIMENTAL PROCEDURE

A. HEAT TRANSFER EXPERIMENTS

Heat transfer experiments were performed for both water and Brayco Micronic 889 (Castrol) Polyalphaolefin (PAO). Since the purpose of these experiments was to determine the Colburn j factor for varying Reynolds numbers, the flowrate was varied to be able to obtain the desired Reynolds numbers of interest.

The flow velocity (Reynolds number) was limited by the maximum pressure the heat exchanger could withstand. With the power to the heater held constant, the pump speed was varied between 10-70 % of its maximum value which corresponded to Reynolds numbers in the range of 50-650 for water and Reynolds numbers in the range of 10-80 for Brayco Micronic 889 Polyalphaolefin. This procedure was repeated for various power inputs to the heater (100-250 Watts). The power input to the heater was limited to 250 Watts due to precision resistor limitations.

The bath temperature was maintained at around $20^{o}C$. As stated previously, after the system reached the steady state condition, the necessary data was collected by the Data Acquisition Unit and used to determine the heat transfer characteristics of the test section. For the calculations the following steps were followed:

1. Reynolds Number Calculations

All the calculations were based on the hydraulic diameter. The hydraulic diameter relates the cross-sectional area of a channel to its heat transfer area. For the present study different area definitions were defined to determine the hydraulic diameter and the Reynolds number.

- Channel Cross Sectional Area (A_c) :

The product of the fin height h, and the fin spacing s, gives the cross-sectional area of each channel.

$$A_c = s \times h \qquad \text{Equation 3.1}$$

- Total Cross Sectional Area (A_f) :

The total cross sectional area of the test section can be obtained by multiplying the number of channels M in the array with A_c. There are nineteen and a half channels along the first fin row.

$$A_f = M \times A_c \qquad \text{Equation 3.2}$$

- Heat Transfer Area (A) :

The heat transfer area of a channel can be determined by using the following formula where h is the fin height, l is the fin length and t is the fin thickness.

$$A = 2 \times (h \times l) + 2 \times (t \times h) + s \times l \qquad \text{Equation 3.3}$$

Since the plexiglas cover is not considered a heat transfer surface, the channel length was modeled in Equation 3.3 as an uncovered channel, and included the blunt edges of the alternating fins.

- Test Section Heated Area (A_h) :

The effective area of the heater was defined as the heated area which is actually 0.07742 m^2.

For the present study the hydraulic diameter was defined as follows ;

$$D_h = \frac{4A_c}{A/l} \qquad \text{Equation 3.4}$$

A/l represents the characteristics length of each channel. As stated previously, the volumetric flow rate, Q was determined by using the flowmeter calibration curves obtained for both water and Brayco Micronic 889 Polyalphaolefin. (See Appendix A). Dividing the volumetric flow rate by the total cross-sectional area A_f, the velocity V through the channels was determined.

$$V = \frac{Q}{A_f} \qquad \text{Equation 3.5}$$

The fluid properties were determined by using the film temperature, T_f. The density ρ, viscosity μ, specific heat C_p, thermal conductivity k_f and Prandtl number P_r of water taken from Ref. 9 were curve fitted in the range of 0-80 ^oC.The same procedure was repeated for Brayco Micronic 889 Polyalphaolefin. The properties of this coolant are tabulated as Appendix C according to the data provided by the manufacturer, Castrol [Ref.. 10].

Finally the Reynolds number based on the hydraulic diameter was determined as follows;

$$Re_D = \frac{\rho \times D_h \times V}{\mu} \qquad \text{Equation 3.6}$$

2. Colburn j Factor Calculations

The film temperature T_1, was averaged between the plate average temperature T_{avg}, and the coolant inlet temperature T_{in}. As explained in the section about thermocouples, the inlet temperature of the coolant was measured at four locations. The plate average temperature was the average temperature of the 23 thermocouples which were placed between the heater pad and the base plate.

$$T_f = \frac{T_{avg} + T_{in}}{2} \qquad \text{Equation 3.7}$$

$$T_{in} = \frac{T_{412} + T_{413} + T_{414} + T_{415}}{4} \qquad \text{Equation 3.8}$$

$$T_{avg} = \frac{T_{(100-111)} + T_{(400-410)}}{23}$$ Equation 3.9

(The subscript numbers of T in Equations 3.8 and 3.9 represent the thermocouple numbers).

The electrical power input P_{elec} to the heater was calculated by using the equations 2.1, 2.2 and 2.3. The temperature difference through the insulation layer ΔT_{insul} used to estimate the heat losses from the heat exchanger.

$$\Delta T_{insul.} = \frac{T_{416} + T_{417} - T_{116} - T_{117}}{2}$$ Equation 3.10

Since the thickness of the insulation t_{insul} was about 0.01905 m and the thermal conductivity k_{insul} was 0.04 W/mK. The lost or gained heat was determined by using the following formula.

$$\Delta P = \frac{k_{insul.} \times \Delta T_{insul.} \times A_h}{t_{insul.}}$$ Equation 3.11

Here A_h represents the area covered with the insulation layer. The actual power P, to the system was obtained by adding ΔP to the electrical power.

$$P = P_{elec.} + \Delta P$$ Equation 3.12

The next step was to calculate the heat flux. Since the heater dimensions and the power input to the heater was held constant for a set of experiments, the heat flux q'' was also constant. The heat flux and the average Nusselt number Nu_{avg} were calculated as follows:

$$q'' = \frac{P}{A_h}$$ Equation 3.13

$$Nu_{avg} = \frac{q'' \times D_h}{k_f \times (T_{avg} - T_{in})}$$ Equation 3.14

Finally, the experimental Colburn j factor was calculated to relate the dimensionless heat transfer coefficient to the Reynolds number.

$$j = \frac{Nu_{avg}}{Re_D \times \mathrm{Pr}^{1/3}}$$ Equation 3.15

B. FLOW VISUALIZATION EXPERIMENTS

The procedure for these experiments was to change the flow velocity of the water and visualize the flow on the offset strip fins. Only water was used as the working fluid and the power input to the heater was set to zero during the visualization experiments. The pump speed was varied to obtain the same Reynolds numbers of the heat transfer experiments performed with water (Re 50-650). Each fin row was labeled on the plexiglass cover to be able to determine the location of the changes in the velocity profile. First blue ink and then white dye were injected into the plexiglas cover and directed through the fin array. Photographs were taken for each Reynolds number settings. Several photographs should be taken to be able to observe all the fin rows.

IV. RESULTS

A. HEAT TRANSFER RESULTS

When water was used as the working coolant the power supply was set to 100, 150, 200 and 250 Watts. The data obtained and the calculated Colburn j factors are tabulated for each power setting in Tables 1-4. Also some of the experimental data were plotted for varying Reynolds numbers and power inputs.

The differences between the water inlet, and water outlet temperatures are plotted on a graph (Figure 13), while the differences between the average plate and water inlet temperatures are plotted on another graph (Figure 14), for all power settings. Figure 15, shows the plate average temperatures for varying Reynolds numbers. The calculated Colburn j factors are also plotted separately for each power setting in Figures 16-19.

The same procedure was repeated for the coolant Brayco Micronic 889 Polyalphaolefin. This time the power supply was set to 100, 175 and 250 Watts. The data obtained were tabulated in Tables 5-7. Temperature differences mentioned above are plotted in Figures 20 and 21. The calculated Colburn j factors for the coolant PAO are shown in Figures 22-24. The correlations developed by Weiting [Ref. 3], and Manglik and Bergles [Ref. 4], were used to predict the Colburn j factor for the present study. (See Chapter I, Section C). These predicted Colburn j factors were plotted in Figures 25-28 to be able to compare with the experimental results obtained for various power inputs. These figures also included the results for the coolant PAO to determine the Prandtl number effect on the Colburn j factor. It was noted that the Prandtl number of the PAO (Brayco Micronic 889) was around 230-250 and the Prandtl number of water was around 5-7 during the experiments.

The data and the graphs showed that as the Reynolds number increased, the Nusselt number also increased for both of the coolants. It was noted that higher power inputs produced higher Nusselt numbers. For the same power input and Reynolds

number, the coolant Brayco Micronic 889, produced significantly higher Nusselt numbers than water.

As the Reynolds number increased, the temperature difference between the inlet and outlet of the heat exchanger showed an exponential decrease for all power settings. Since the inlet temperature of the coolant was maintained at a constant temperature (around 20 ^{o}C), for the same Reynolds number as the power input increased the temperature difference mentioned above also increased.

As the power input increased, the average surface temperature of the base plate increased. But increasing the Reynolds number decreased the plate average temperature and also decreased the difference between the plate average and coolant inlet temperatures. Since the volume of the circulating bath was small, as the Reynolds number exceeded about 650 for water and about 60 for the PAO, the inlet temperature of the coolant and the plate average temperature began to increase. When the coolant was the PAO, for the Reynolds numbers greater than 60, the maximum increase in the plate average temperature was less than 0.60 ^{o}C.

It was noted that, even though the variation was very small, higher power inputs produced higher Colburn j factors for the same Reynolds number settings. As the power input increased the plate average temperature and the coolant film temperature also increased. This caused a decrease in the Prandtl number and an increase in the Colburn j factor. The predicted Colburn j factors developed by Weiting [Ref. 3], and Manglik and Bergles [Ref. 4], were compared to the experimental results. When the water was used as the working fluid, there was a very close agreement with the results of these studies. Especially, when the Reynolds number was less than 200, the experimental results were in the accuracy zone of Weiting (± 10 %), and Manglik and Bergles (± 20 %). For the Reynolds numbers greater than 200, the experimental results deviated slightly from the accuracy zone. The maximum deviation was 38.20 %, when the power input was minimum (100 Watts), and 29.93 %, when the power input was maximum (250 Watts). For the power input of 250 Watts, about half of the experimental results were in the

accuracy zone. The difference between the predicted and calculated Colburn j factors for the power input of 250 Watts were tabulated in Table 8.

Since the predictive correlations were applicable for Prandtl numbers in the range of 0.5 to 15, and the Prandtl number of Brayco Micronic 889 (PAO), was about 230-250 during the experiments, there was not a close agreement between the predicted and experimental results when this coolant (PAO) was used as the working fluid. Even though the experimental results were higher than the predicted values the curves obtained for both of the experimental and predicted Colburn j factors showed a similar tendency. (See Figures 25-28). This validated the Prandtl number limitations of these predicted correlations.

Finally, the Colburn j factors of water and Brayco Micronic 889 (PAO) were compared to each other. When the power input was 250 Watts and the Reynolds number was around 57, the calculated Colburn j factor was 0.0856 for water (Pr = 6.03), and 0.3280 for the PAO (Pr = 238.72), it was noted that the ratio between the Colburn j factors was about the same to the 1/3 to the power of the ratio between the Prandtl numbers.

$$\frac{j_{PAO}}{j_{water}} = \frac{0.3280}{0.0856} = 3.83$$

$$\left(\frac{\mathrm{Pr}_{PAO}}{\mathrm{Pr}_{water}}\right)^{1/3} = \left(\frac{238.72}{6.03}\right)^{1/3} = 3.41$$

The difference between the ratios was about 11 %.

Power Input=100 Watts (Heat Flux ≅ 1290 W/m²)

Re	T1 (Inlet Temp.) (°C)	T2 (Outlet Temp) (°C)	T3 (Avg Plate) (°C)	T2-T1 (°C)	T3-T1 (°C)	△P (Watts)	Nu	j
53.01	20.22	20.80	25.03	0.58	4.81	0.453	7.35	0.0743
142.19	20.35	20.74	24.91	0.39	4.56	0.476	7.76	0.0292
186.11	20.28	20.62	24.70	0.34	4.42	0.480	8.01	0.0230
229.61	20.25	20.55	24.42	0.30	4.17	0.483	8.49	0.0198
273.12	20.18	20.43	24.28	0.25	4.10	0.488	8.64	0.0169
315.65	20.05	20.26	24.02	0.21	3.97	0.502	8.94	0.0151
359.23	20.06	20.24	23.94	0.18	3.88	0.515	9.15	0.0136
402.83	20.09	20.23	23.86	0.14	3.77	0.533	9.42	0.0125
447.02	20.19	20.30	23.82	0.11	3.63	0.546	9.78	0.0117
490.96	20.26	20.36	23.76	0.10	3.50	0.560	10.13	0.0110
534.35	20.27	20.36	23.68	0.09	3.41	0.574	10.40	0.0104
576.23	20.18	20.26	23.51	0.08	3.33	0.592	10.67	0.0099

Table 1. Experimental Data for Water (Power Input = 100 W).

Power Input=150 Watts (Heat Flux ≅ 1940 W/m²)

Re	T1 (Inlet Temp.) (°C)	T2 (Outlet Temp) (°C)	T3 (Avg Plate) (°C)	T2−T1 (°C)	T3−T1 (°C)	△P (Watts)	Nu	j
54.21	20.11	20.96	26.89	0.85	6.78	0.527	7.83	0.0779
150.40	20.00	20.59	26.11	0.59	6.11	0.592	8.69	0.0325
188.58	20.02	20.52	25.98	0.50	5.96	0.605	8.93	0.0255
232.81	19.95	20.39	25.79	0.44	5.84	0.611	9.11	0.0210
277.32	19.95	20.33	25.69	0.38	5.74	0.619	9.28	0.0180
321.81	19.98	20.31	25.58	0.33	5.60	0.629	9.51	0.0159
365.99	19.94	20.22	25.50	0.28	5.56	0.074	9.60	0.0141
410.64	19.97	20.24	25.46	0.26	5.49	0.631	9.72	0.0127
455.44	20.06	20.29	25.39	0.23	5.33	0.631	10.00	0.0118
498.72	20.06	20.26	25.17	0.20	5.11	0.629	10.45	0.0112
543.72	20.17	20.35	25.12	0.18	4.95	0.631	10.77	0.0106
587.64	20.17	20.34	25.03	0.17	4.86	0.632	10.96	0.0100

Table 2. Experimental Data for Water (Power Input = 150 W).

Power Input=200 Watts (Heat Flux ≅ 2580 W/m^2)

Re	T1 (Inlet Temp.) (°C)	T2 (Outlet Temp) (°C)	T3 (Avg Plate) (°C)	T2−T1 (°C)	T3−T1 (°C)	△P (Watts)	Nu	j
56.03	20.50	21.66	29.10	1.16	8.60	0.390	8.16	0.0795
149.19	20.67	21.50	28.35	0.83	7.68	0.475	9.15	0.0334
195.36	20.63	21.36	28.14	0.73	7.51	0.478	9.38	0.0261
241.66	20.63	21.27	28.03	0.64	7.40	0.483	9.52	0.0214
287.54	20.58	21.14	27.89	0.56	7.31	0.484	9.63	0.0182
333.41	20.61	21.09	27.72	0.48	7.11	0.493	9.92	0.0161
379.60	20.68	21.12	27.61	0.44	6.93	0.494	10.17	0.0146
425.53	20.71	21.10	27.50	0.39	6.79	0.494	10.39	0.0132
472.07	20.81	21.17	27.44	0.36	6.63	0.503	10.64	0.0122
518.14	20.88	21.24	27.33	0.33	6.45	0.507	10.91	0.0114
562.16	20.82	21.14	27.07	0.32	6.25	0.515	11.27	0.0109
606.96	20.86	21.17	26.86	0.31	6.00	0.519	11.74	0.0105

Table 3. Experimental Data for Water (Power Input = 200 W).

Power Input=250 Watts (Heat Flux ≅ 3230 W/m²)

Re	T1 (Inlet Temp.) (°C)	T2 (Outlet Temp) (°C)	T3 (Avg Plate) (°C)	T2−T1 (°C)	T3−T1 (°C)	△P (Watts)	Nu	j
57.04	20.59	22.01	30.44	1.42	9.85	0.543	8.89	0.0856
152.41	20.65	21.68	30.07	1.03	9.42	0.548	9.31	0.0335
199.61	20.62	21.53	29.86	0.91	9.24	0.554	9.50	0.0261
246.24	20.56	21.39	29.59	0.83	9.03	0.564	9.71	0.0216
292.56	20.57	21.31	29.27	0.74	8.70	0.569	10.09	0.0189
338.04	20.49	21.16	28.93	0.67	8.44	0.577	10.41	0.0168
384.29	20.50	21.09	28.76	0.59	8.26	0.590	10.65	0.0151
430.94	20.60	21.13	28.61	0.53	8.01	0.602	10.99	0.0139
477.48	20.64	21.11	28.51	0.47	7.87	0.615	11.16	0.0127
523.55	20.72	21.14	28.31	0.42	7.59	0.632	11.58	0.0121
570.20	20.81	21.20	28.20	0.39	7.39	0.642	11.91	0.0114
614.56	20.74	21.12	27.96	0.38	7.22	0.645	12.20	0.0108

Table 4. Experimental Data for Water (Power Input = 250 W).

Power Input=100 Watts (Heat Flux ≅ 1290 W/m²)

Re	T1 (Inlet Temp.) (°C)	T2 (Outlet Temp) (°C)	T3 (Avg Plate) (°C)	T2-T1 (°C)	T3-T1 (°C)	△P (Watts)	Nu	j
13.48	20.49	23.36	26.17	2.87	5.68	0.410	85.49	1.0096
21.82	20.07	21.96	25.35	1.89	5.28	0.502	92.05	0.6704
30.68	19.92	21.28	24.87	1.36	4.95	0.573	98.27	0.5086
39.41	19.85	20.86	24.47	1.01	4.62	0.645	105.31	0.4240
47.54	19.84	20.59	24.24	0.75	4.40	0.665	110.64	0.3692
54.69	19.89	20.51	24.15	0.62	4.26	0.694	114.27	0.3314
60.59	19.94	20.54	24.10	0.60	4.16	0.696	116.99	0.3062
68.25	20.12	20.65	24.13	0.53	4.01	0.694	121.39	0.2822
71.11	20.54	21.06	24.52	0.52	3.98	0.694	122.38	0.0273

Table 5. Experimental Data for Brayco Micronic 889 (Power Input = 100 W).

Power Input=175 Watts (Heat Flux ≅ 2260 W/m²)

Re	T1 (Inlet Temp.) (°C)	T2 (Outlet Temp) (°C)	T3 (Avg Plate) (°C)	T2−T1 (°C)	T3−T1 (°C)	△P (Watts)	Nu	j
13.69	20.28	25.13	29.56	4.85	9.28	-0.124	91.33	1.0675
22.15	19.92	23.32	28.68	3.40	8.76	0.078	96.85	0.6982
31.08	19.79	22.13	27.74	2.34	7.95	0.171	106.76	0.5476
39.88	19.67	21.55	27.20	1.88	7.53	0.242	112.75	0.4502
48.12	19.75	21.18	26.92	1.43	7.17	0.327	118.46	0.3920
55.38	19.86	21.05	26.87	1.19	7.01	0.347	121.18	0.3484
61.37	19.93	20.98	26.84	1.05	6.91	0.376	122.96	0.3190
69.26	20.32	21.27	27.07	0.95	6.75	0.386	125.89	0.2897
72.13	20.73	21.64	27.37	0.91	6.64	0.378	127.98	0.2831

Table 6. Experimental Data for Brayco Micronic 889 (Power Input = 175 W).

Power Input=250 Watts (Heat Flux ≅ 3230 W/m²)

Re	T1 (Inlet Temp.) (°C)	T2 (Outlet Temp) (°C)	T3 (Avg Plate) (°C)	T2-T1 (°C)	T3-T1 (°C)	△P (Watts)	Nu	j
18.70	20.54	27.64	33.76	7.10	13.22	-0.289	91.46	1.0750
22.73	20.96	25.61	33.01	4.65	12.05	-0.228	100.38	0.7110
31.72	21.14	24.58	32.49	3.44	11.35	-0.125	106.87	0.5421
41.01	21.38	24.03	32.35	2.65	10.97	-0.125	110.57	0.4338
42.83	21.68	23.84	32.32	2.16	10.64	0.007	114.04	0.3684
57.58	22.25	23.97	32.61	1.86	10.36	0.055	117.17	0.3280
64.13	22.92	24.64	33.02	1.72	10.10	0.079	120.20	0.2946
72.42	23.38	24.98	33.27	1.60	9.89	0.072	122.71	0.2739
75.31	23.64	25.15	33.38	1.51	9.74	0.074	124.47	0.2674

Table 7. Experimental Data for Brayco Micronic 889 (Power Input = 250 W).

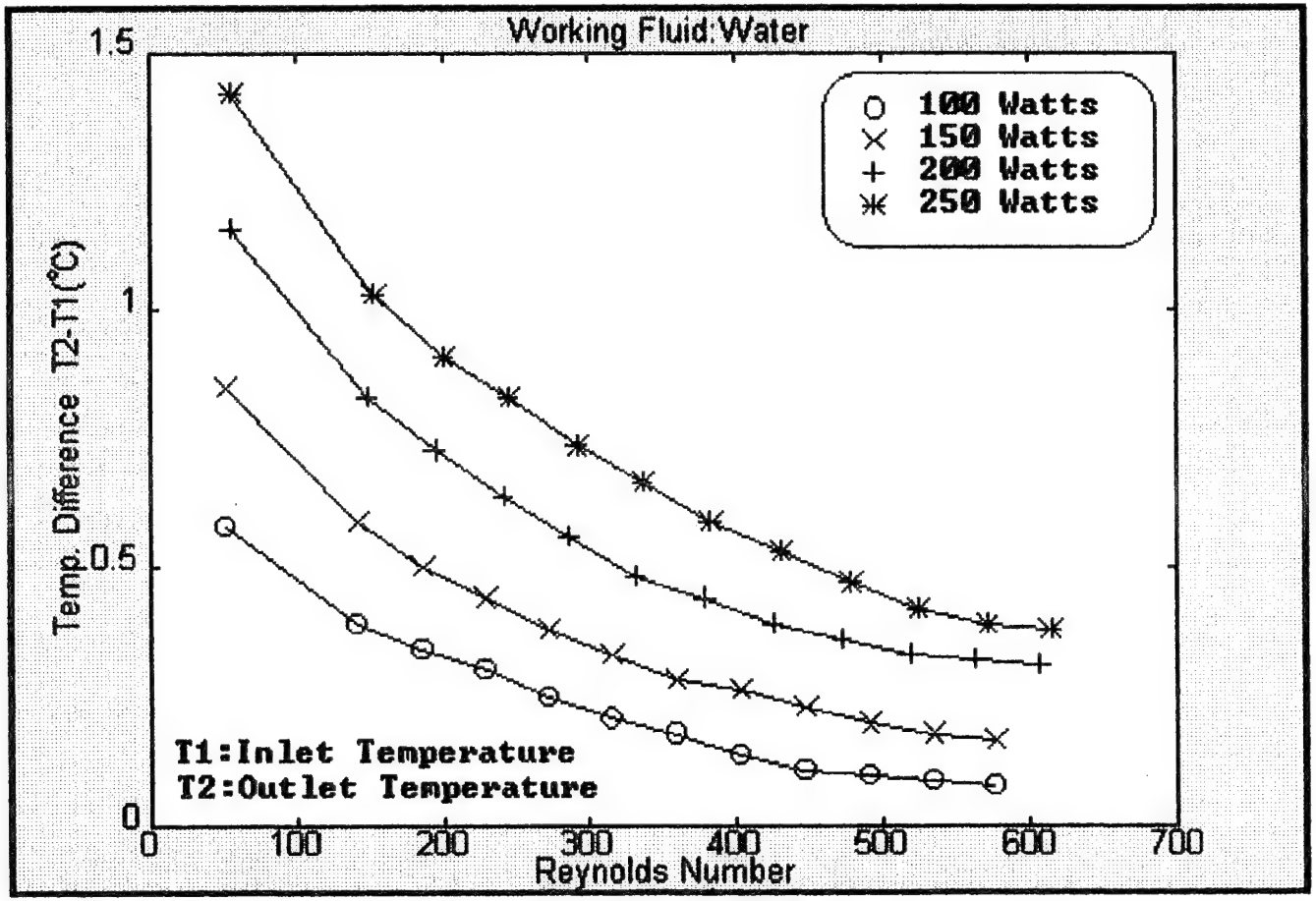

Figure 13. Temperature Difference vs. Reynolds Number.

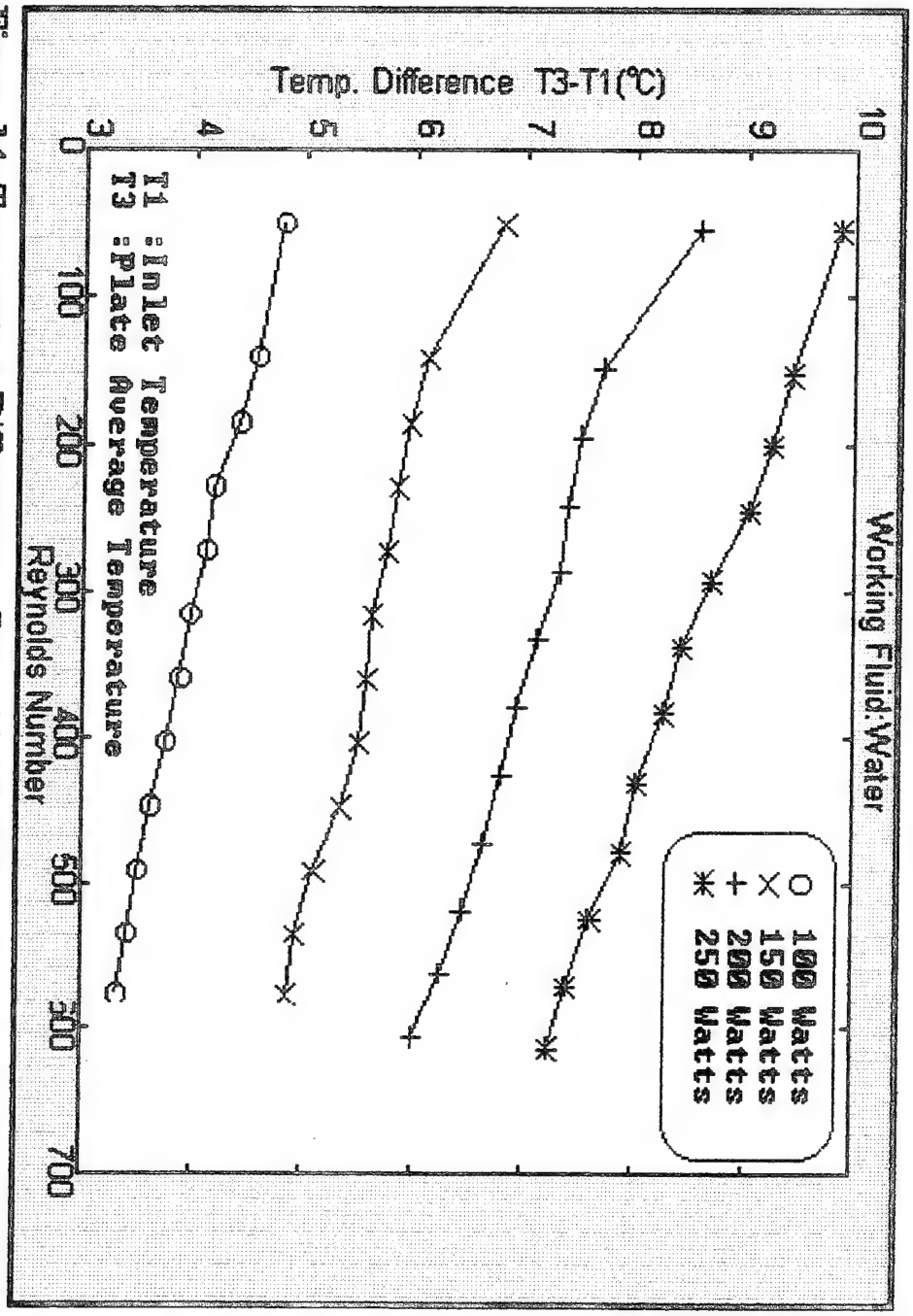

Figure 14. Temperature Difference vs. Reynolds Number.

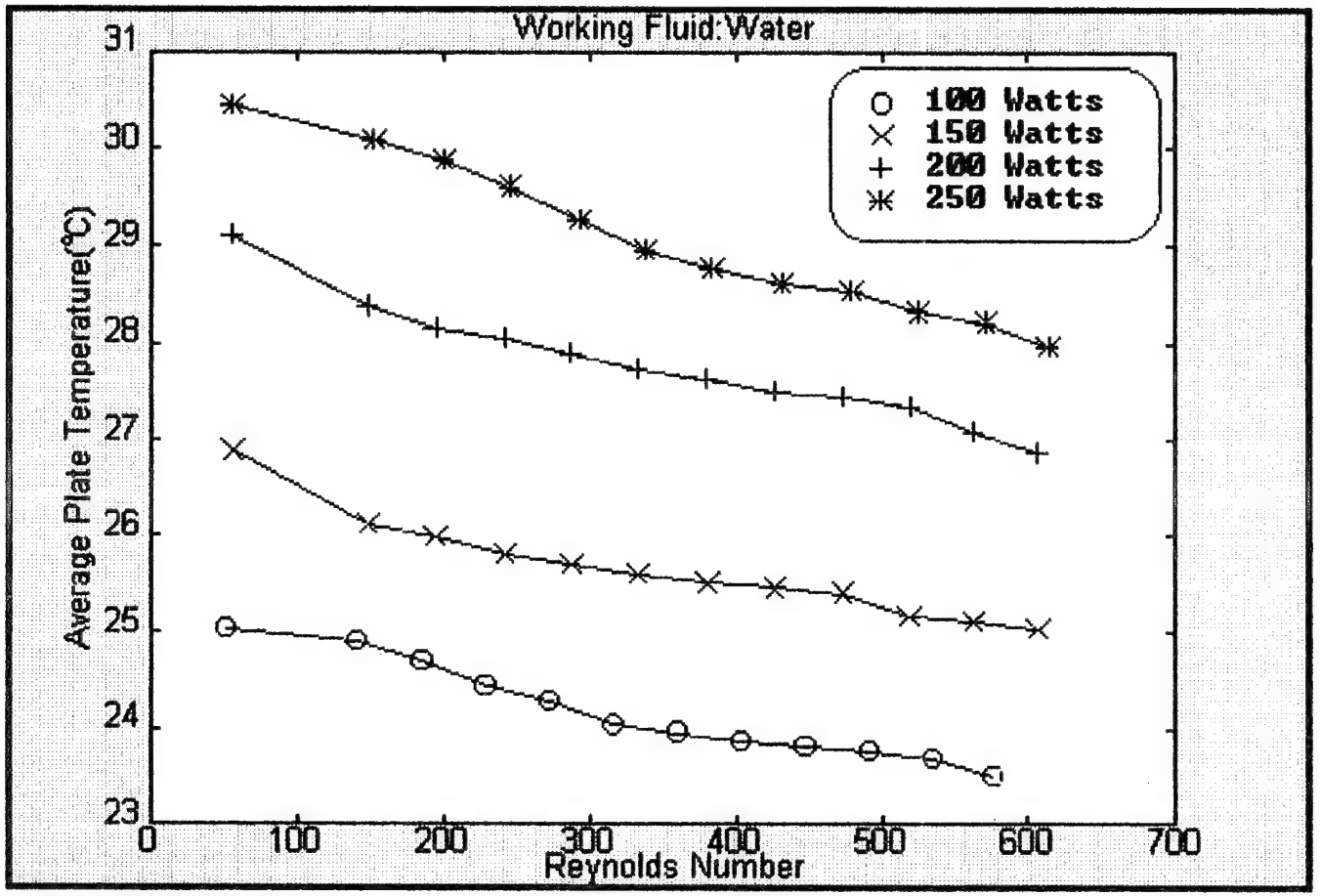

Figure 15. Plate Average Temperature vs. Reynolds Number.

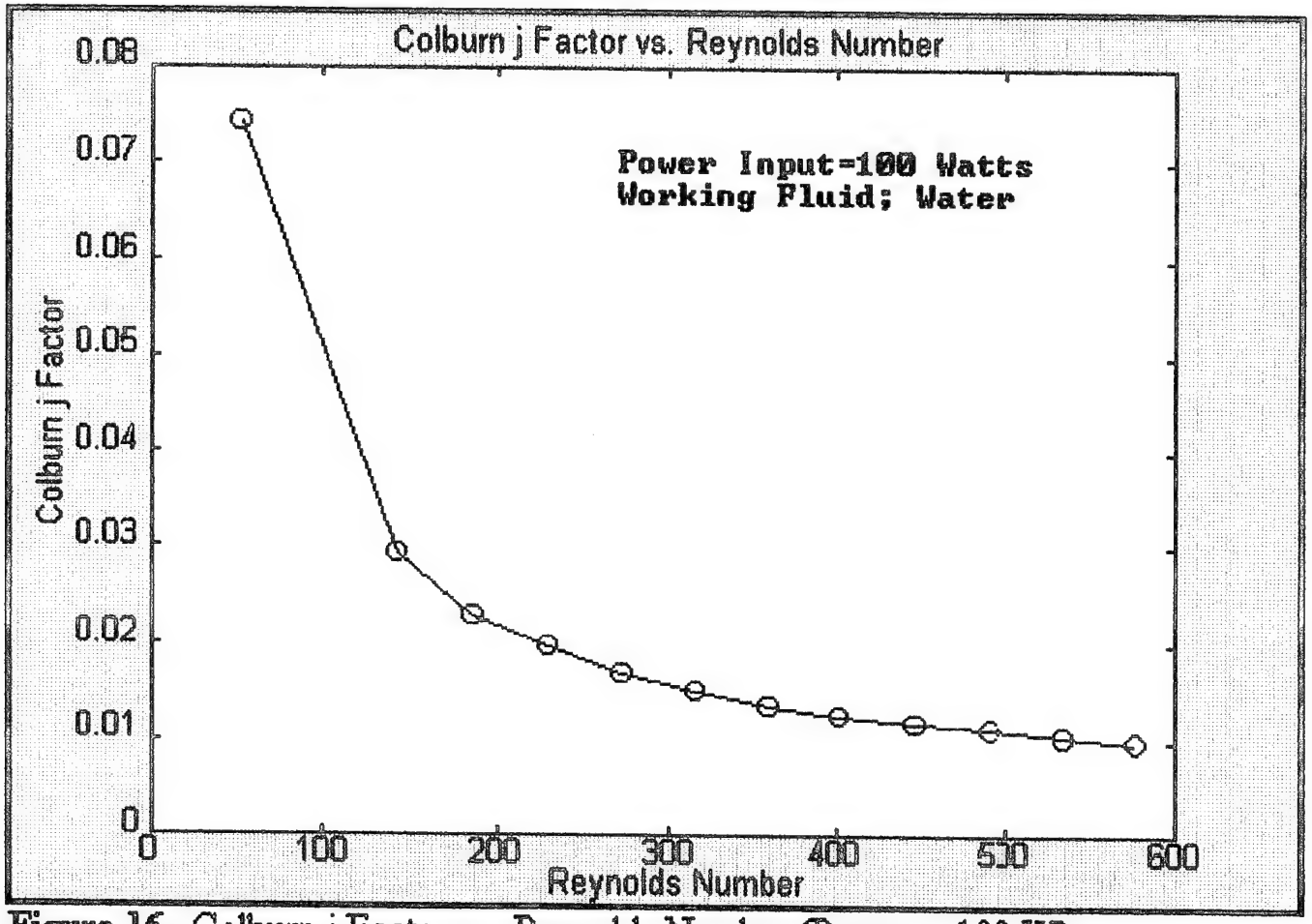

Figure 16. Colburn j Factor vs. Reynolds Number (Power = 100 W).

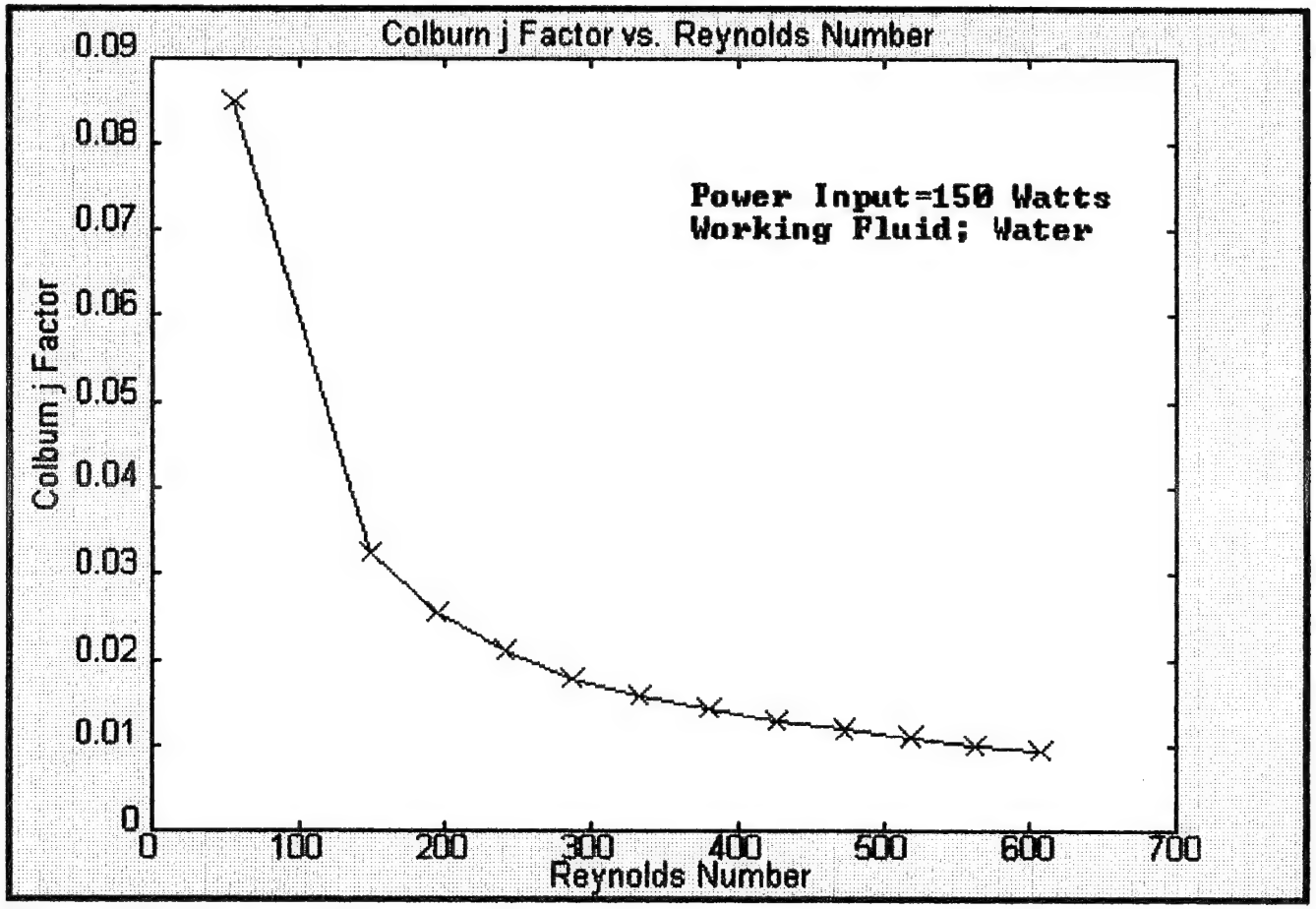

Figure 17. Colburn j Factor vs. Reynolds Number (Power = 150 W).

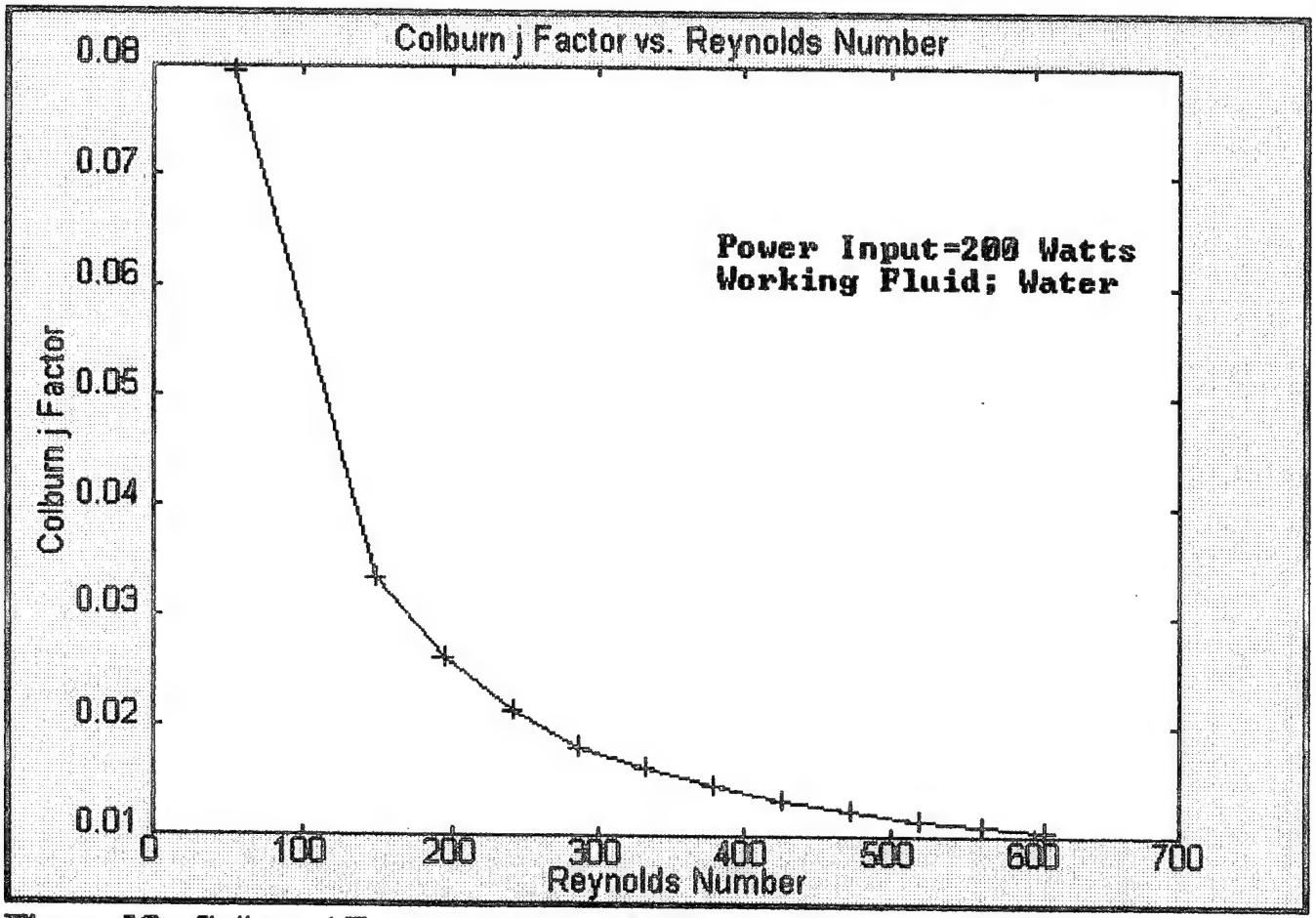

Figure 18. Colburn j Factor vs. Reynolds Number (Power = 200 W).

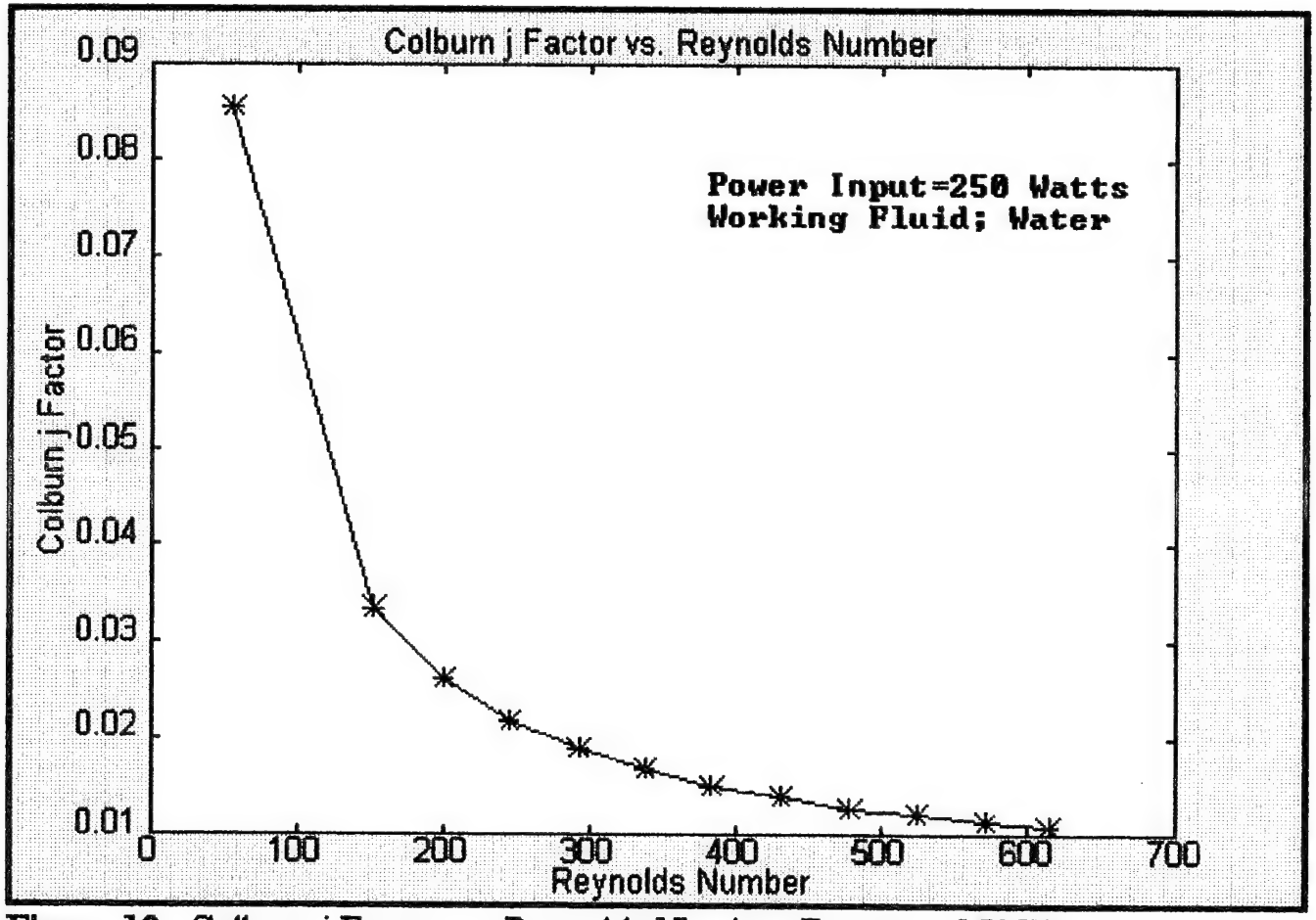

Figure 19. Colburn j Factor vs. Reynolds Number (Power = 250 W).

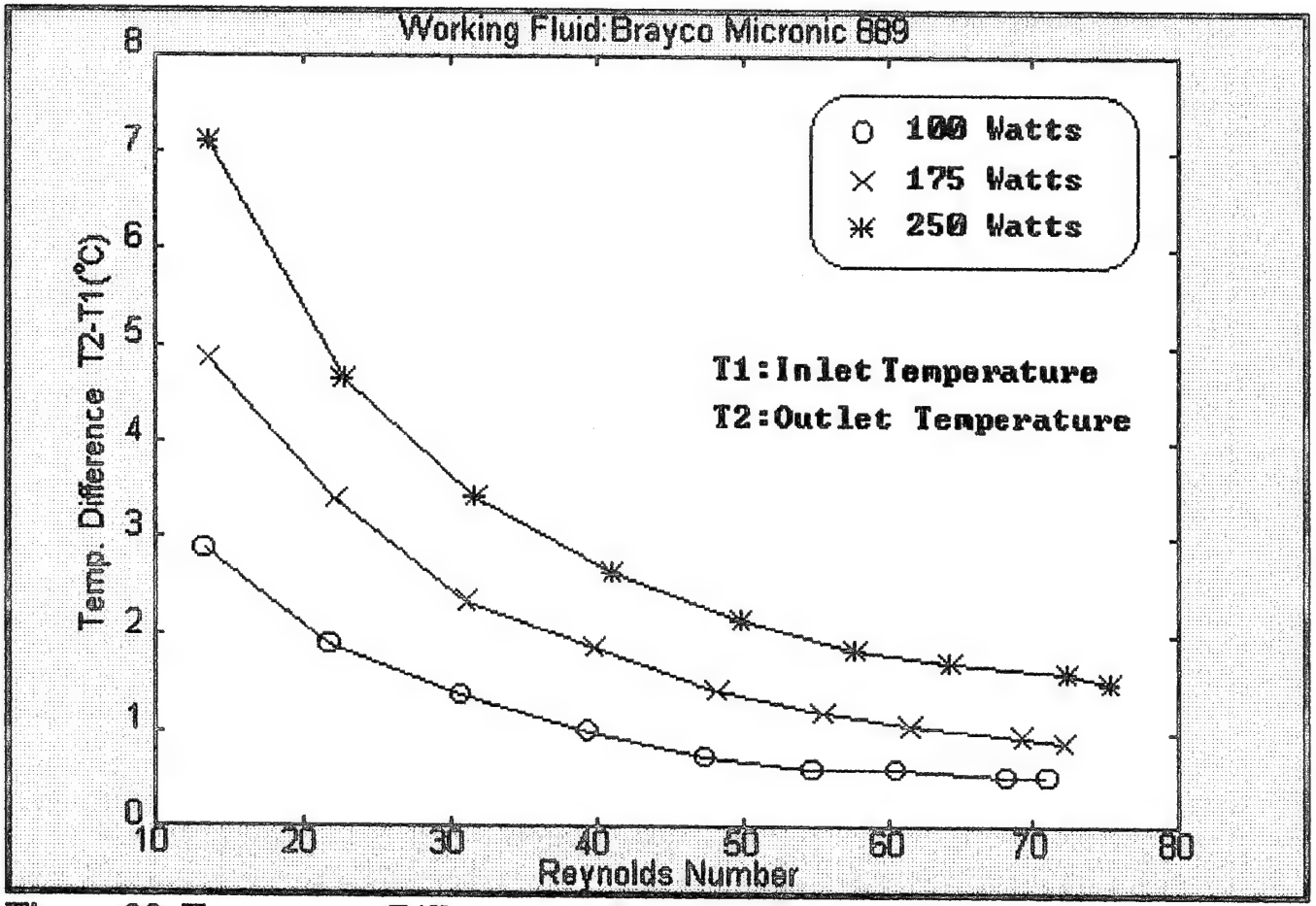

Figure 20. Temperature Difference vs. Reynolds Number.

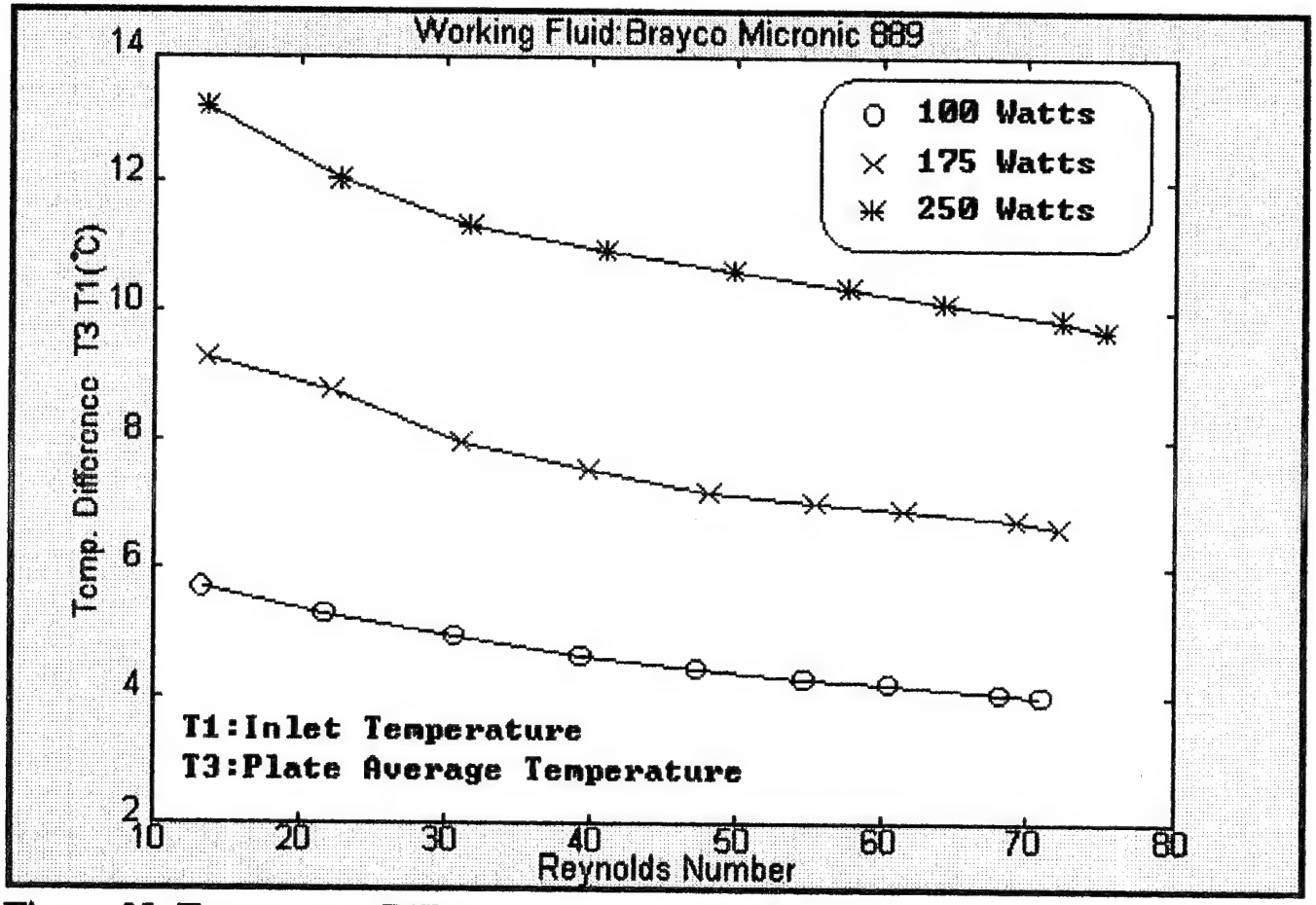

Figure 21. Temperature Difference vs. Reynolds Number.

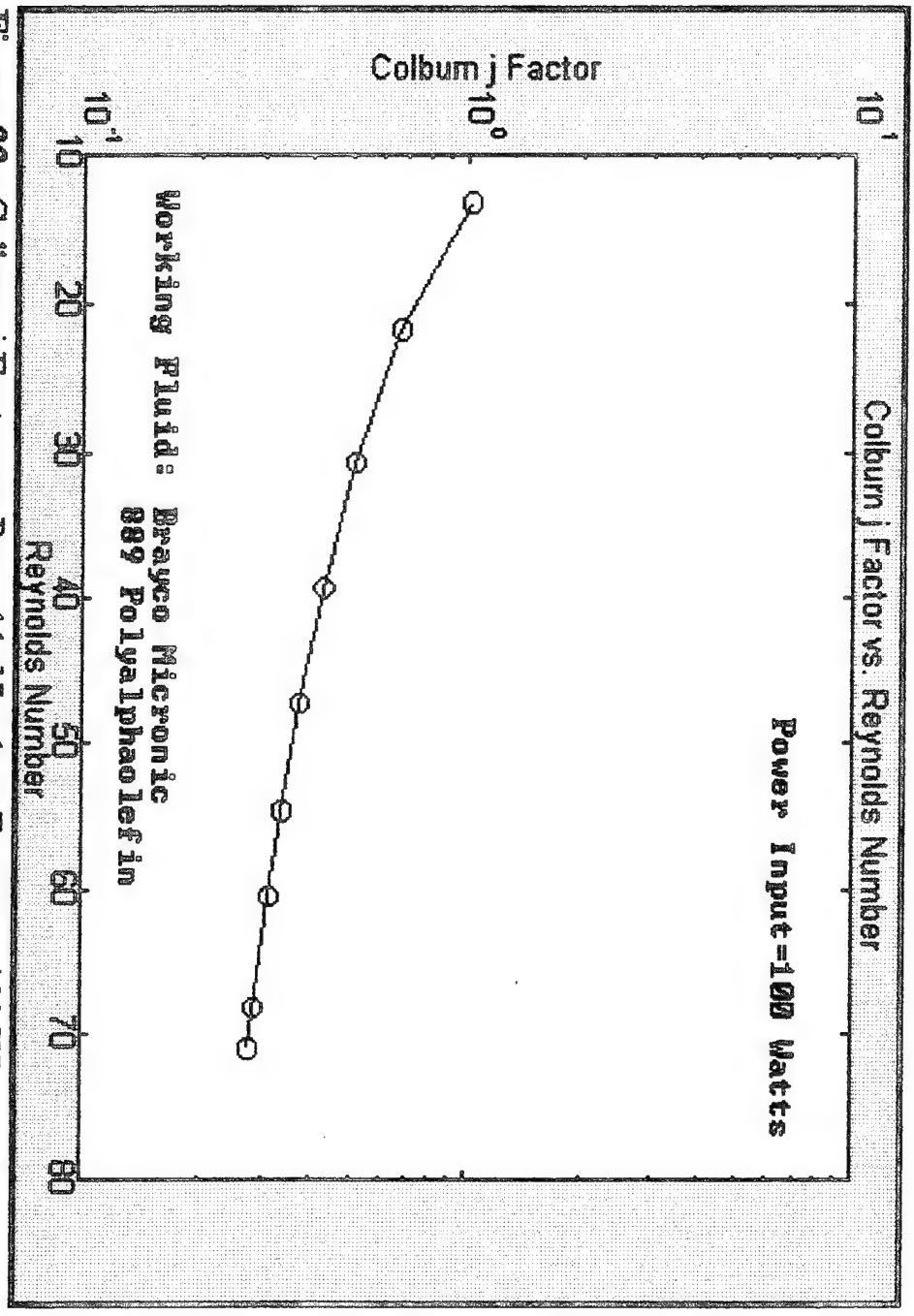

Figure 22. Colburn j Factor vs. Reynolds Number (Power = 100 W).

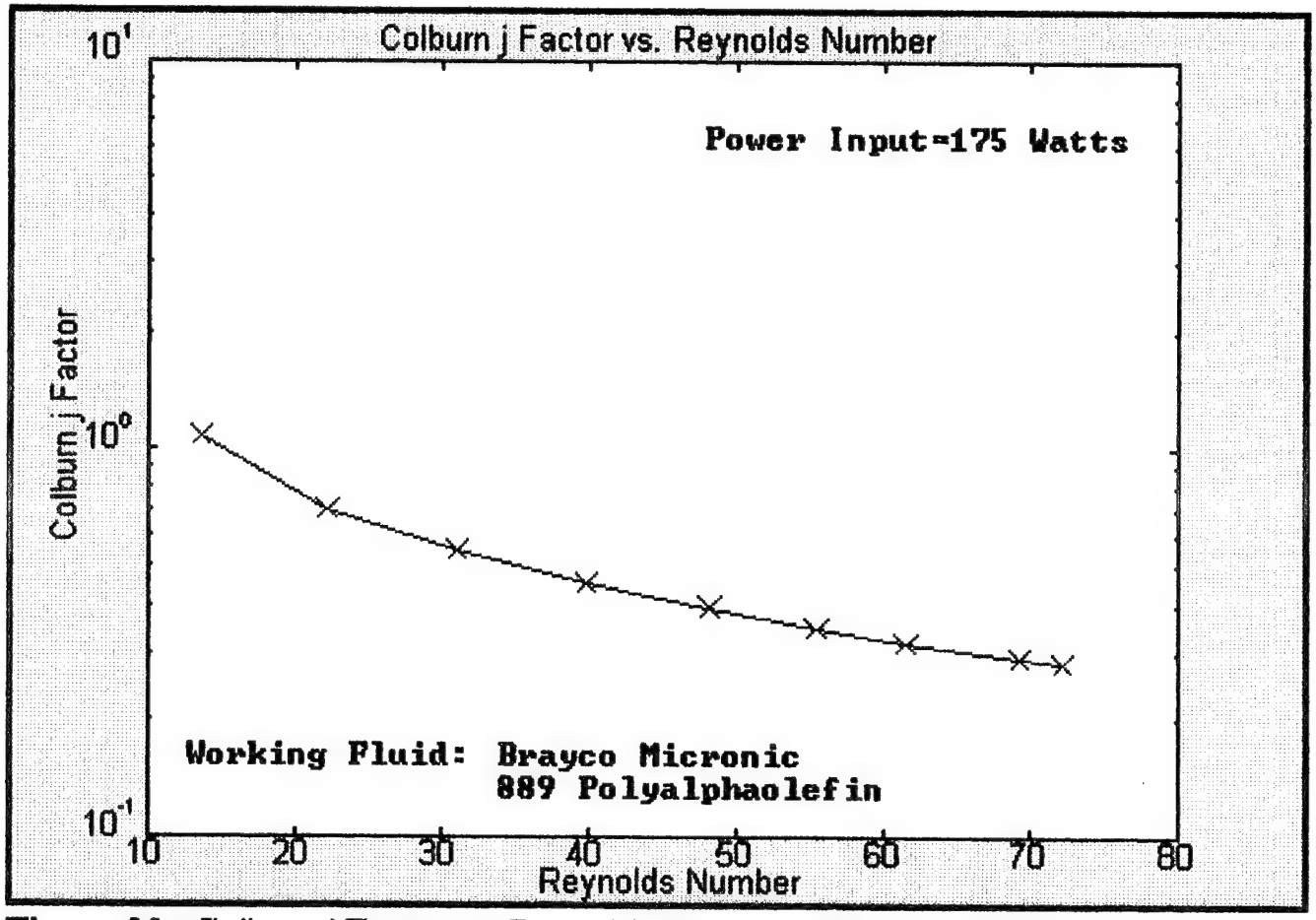

Figure 23. Colburn j Factor vs. Reynolds Number (Power = 175 W).

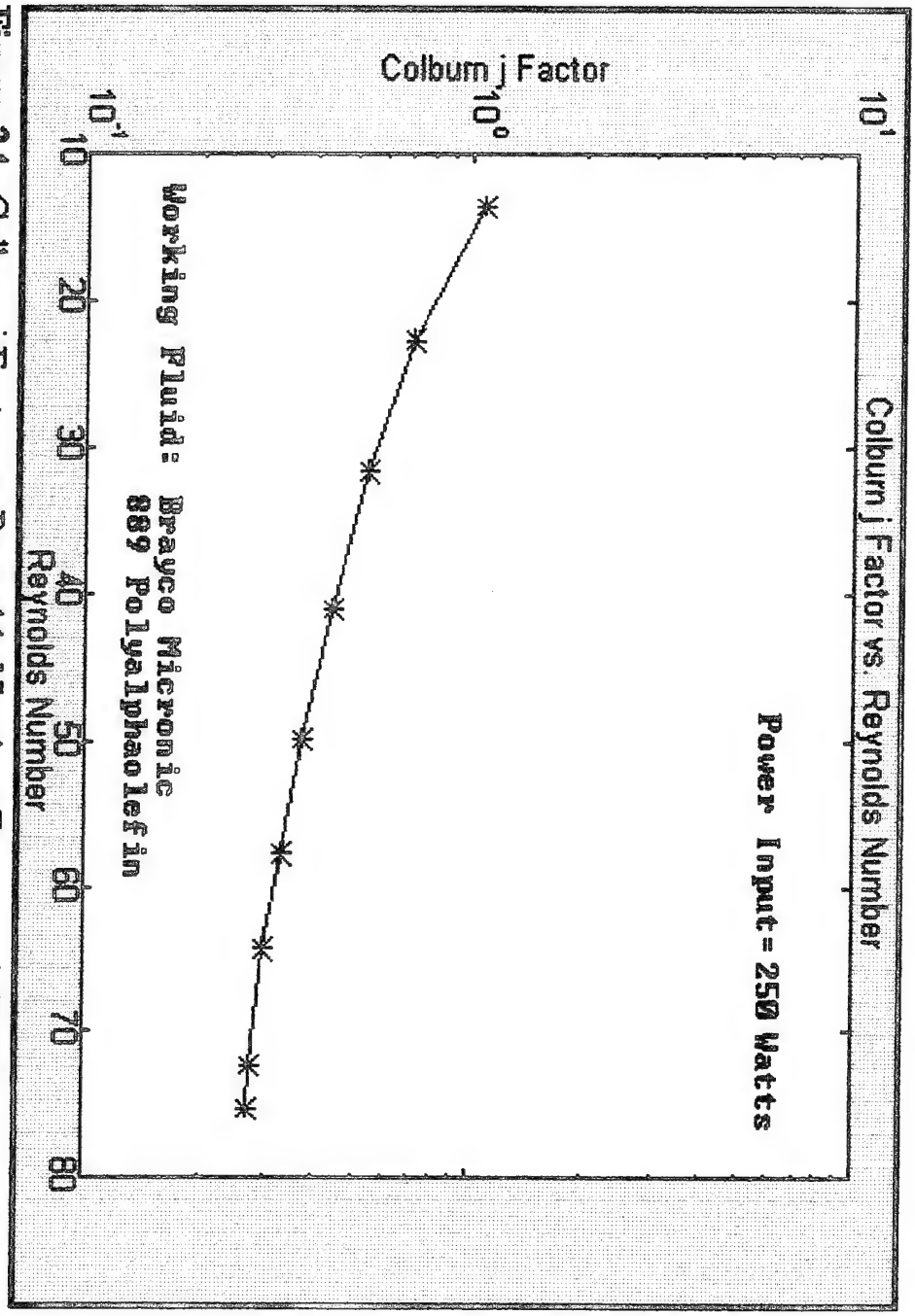

Figure 24. Colburn j Factor vs. Reynolds Number (Power = 250 W).

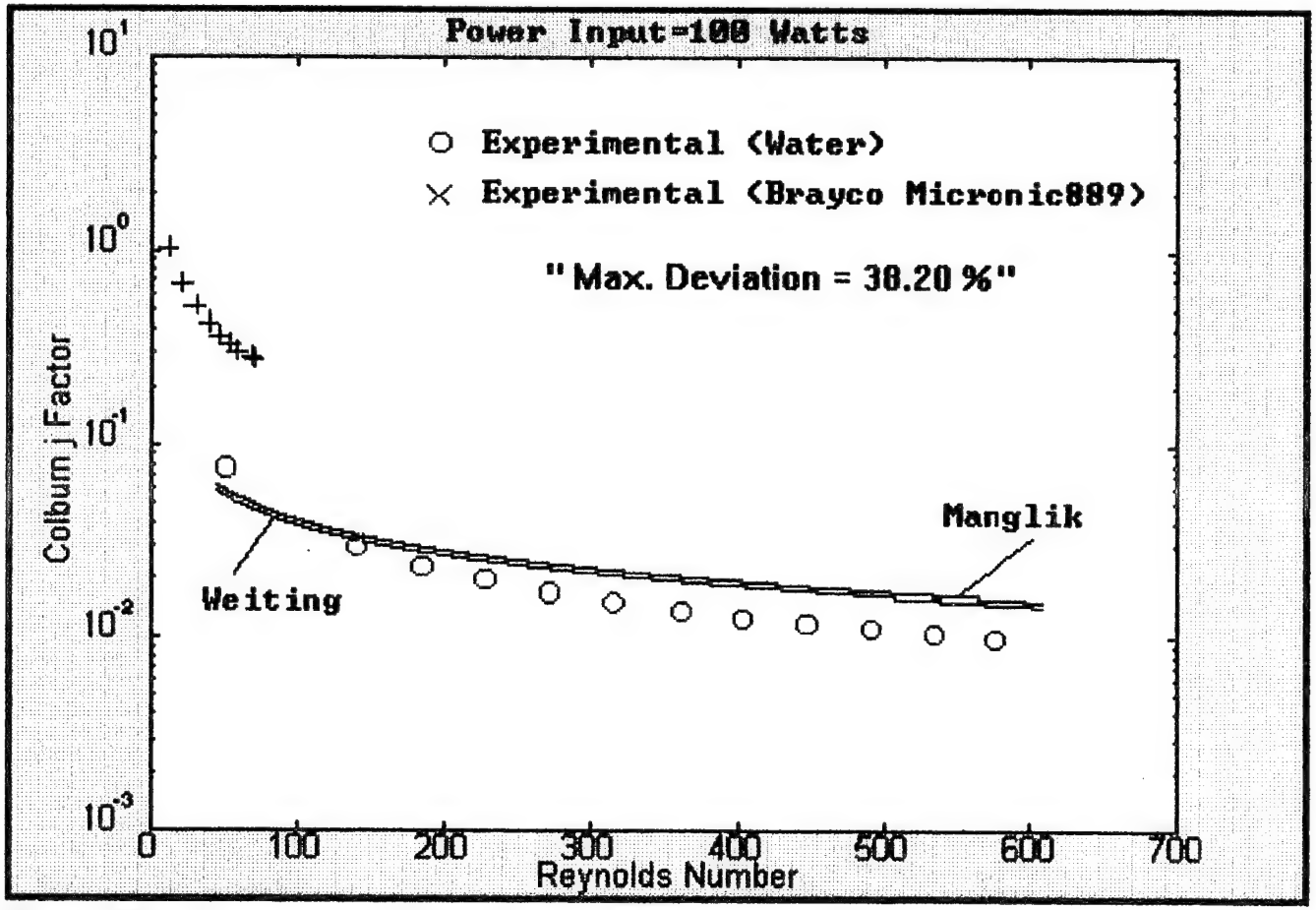

Figure 25. Comparison of Predicted and Experimental j's.

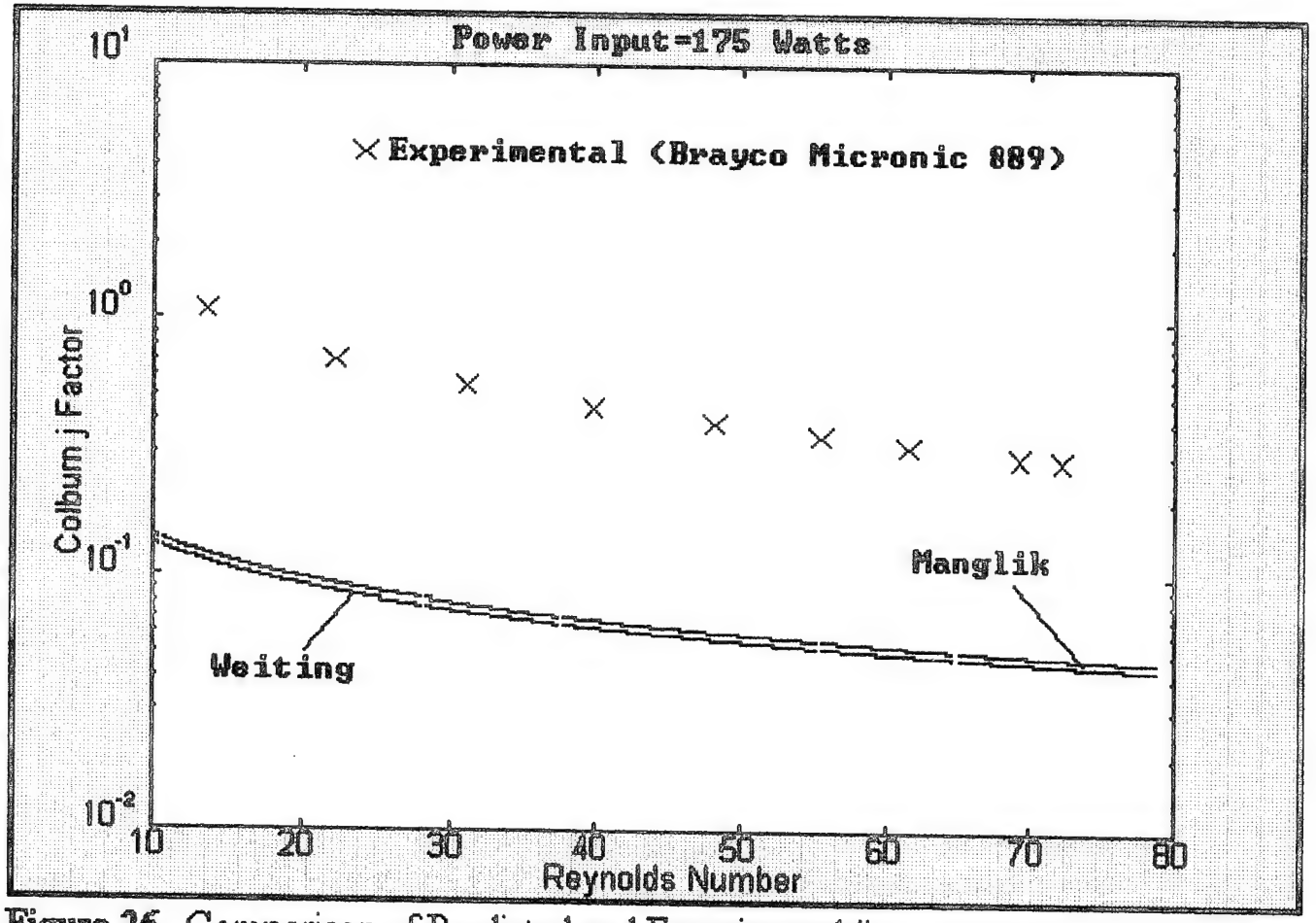

Figure 26. Comparison of Predicted and Experimental j's.

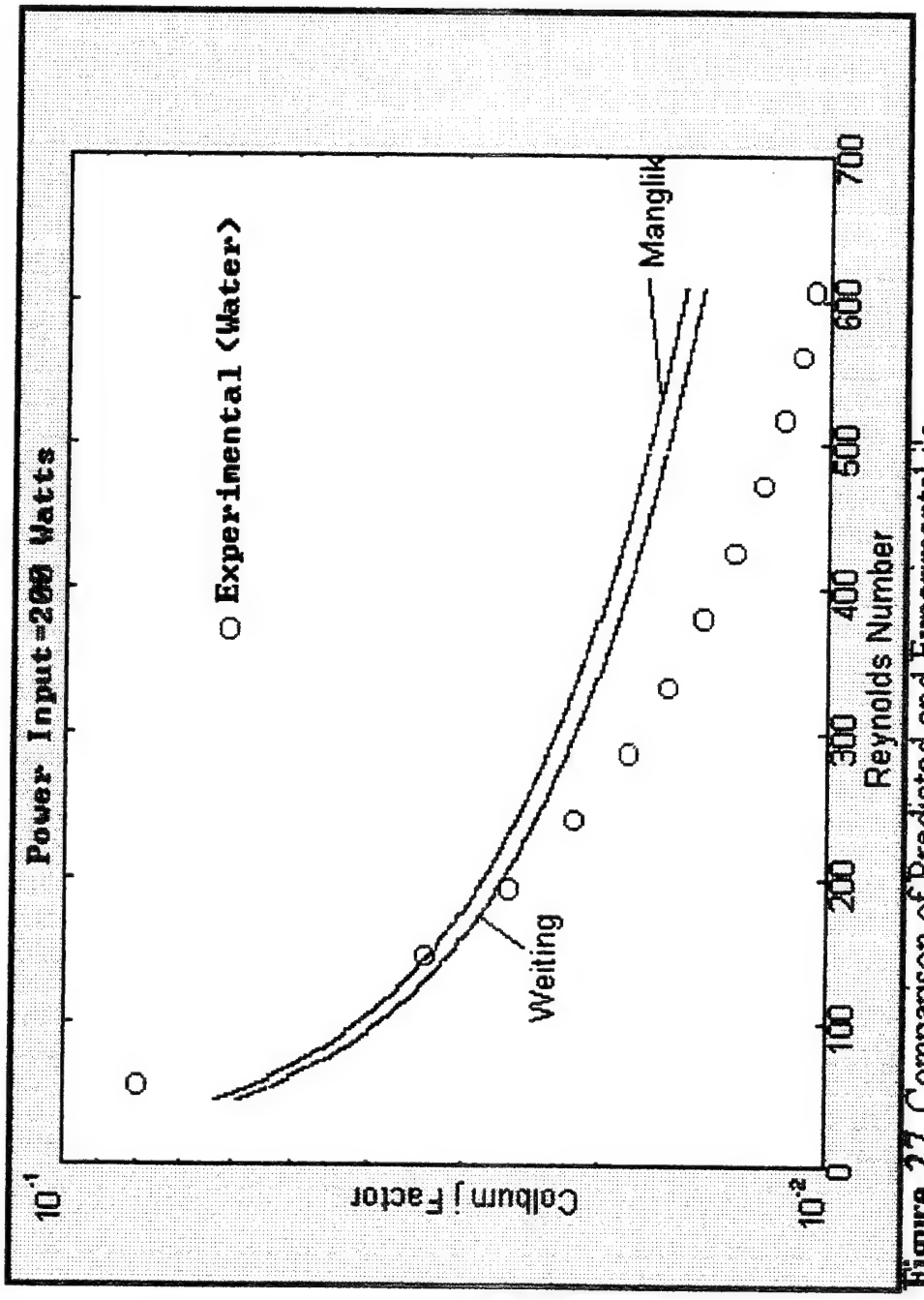

Figure 27. Comparison of Predicted and Experimental j's.

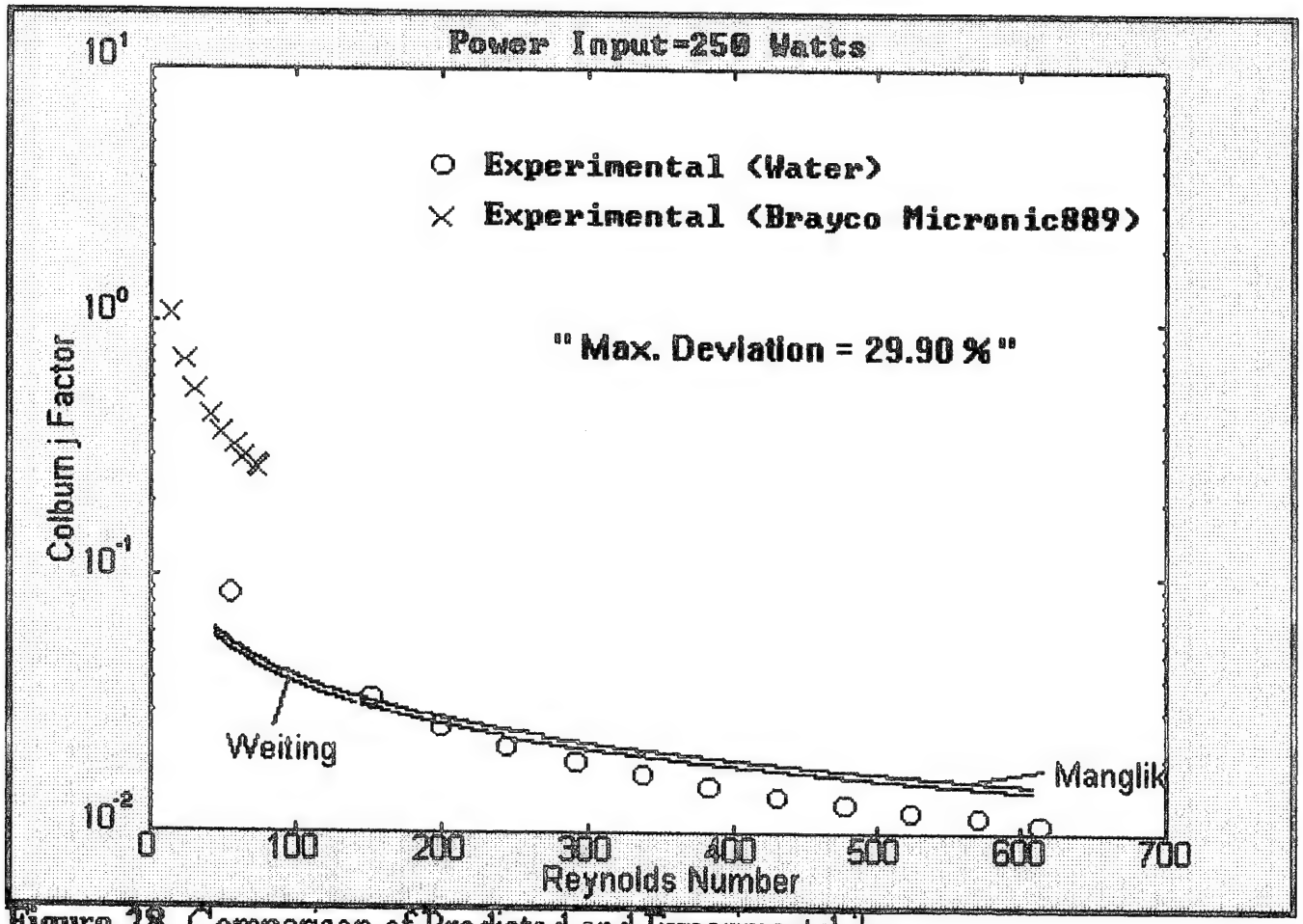

Figure 28. Comparison of Predicted and Experimental j's.

Reynolds Number	j	% Difference (Weiting)	% Difference (Manglik & Bergles)
152.41	0.0335	-8.8705	-2.4176
159.61	0.0261	2.0190	7.7195
246.24	0.0216	9.3036	14.5032
292.56	0.0189	13.1094	18.0300
338.04	0.0168	16.2434	20.9368
384.29	0.0151	19.3857	23.8617
430.94	0.0139	21.1444	25.4860
477.48	0.0127	23.7010	27.8701
523.55	0.0121	24.1215	28.2391
570.20	0.0114	25.0518	29.0929
614.56	0.0108	25.9607	29.9303

Table 8. % Difference Between The Predicted and Calculated j Factors. (Power = 250 W).

B. FLOW VISUALIZATION RESULTS

In this study, a large number of photographs were taken to be able to visualize the flow through the offset strip fins. Two of them were presented in Figures 29 and 30.

When the ink streak was introduced at the leading edge of the fin, the ink followed the side of the fin and did not rise perceptibly from the level of injection. The ink then curled to its center, around the trailing edge of the fin and followed the open channel until reaching the leading edge of the next row. After being deflected by the laminar boundary layer forming on the fin, the flow pattern repeated itself. (See Figures 29 and 30). Since the Reynolds number was limited to 650 by the maximum pressure the heat exchanger could withstand, transition to turbulent and vortices were not observed. But, it was noted that as the Reynolds number increased, the streaklines produced a more severe wavy pattern.

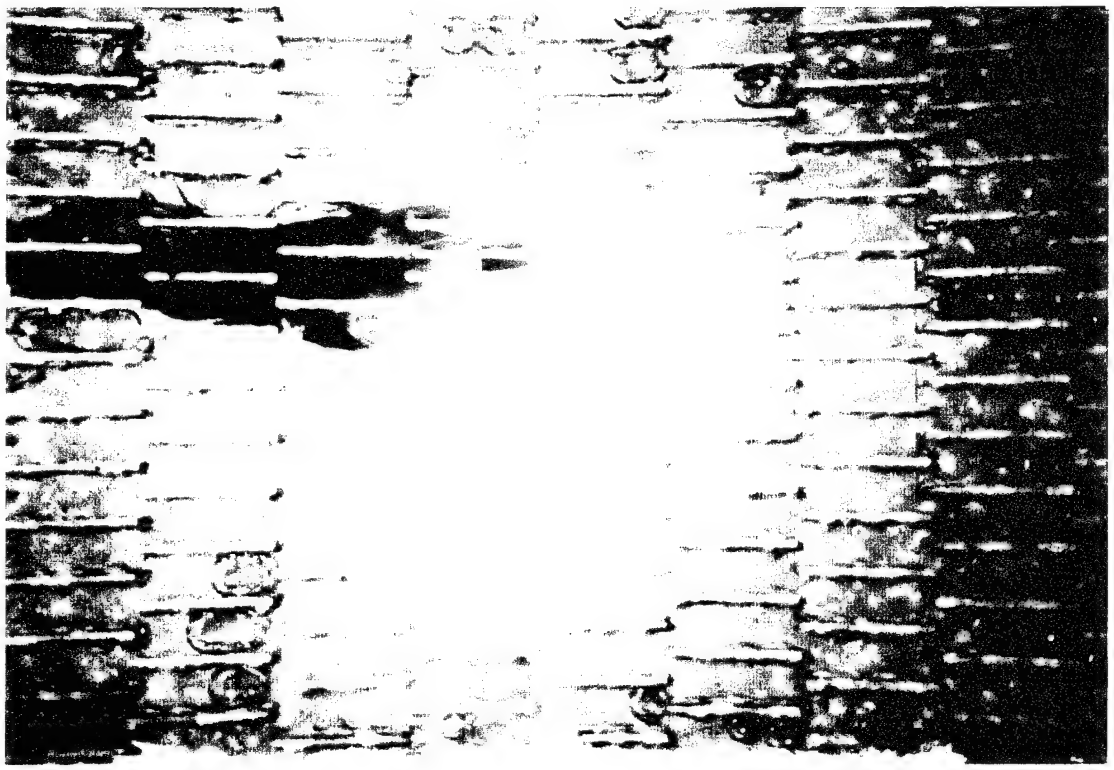

Figure 29. Flow Visualization of Water (Re = 200, First Five Rows).

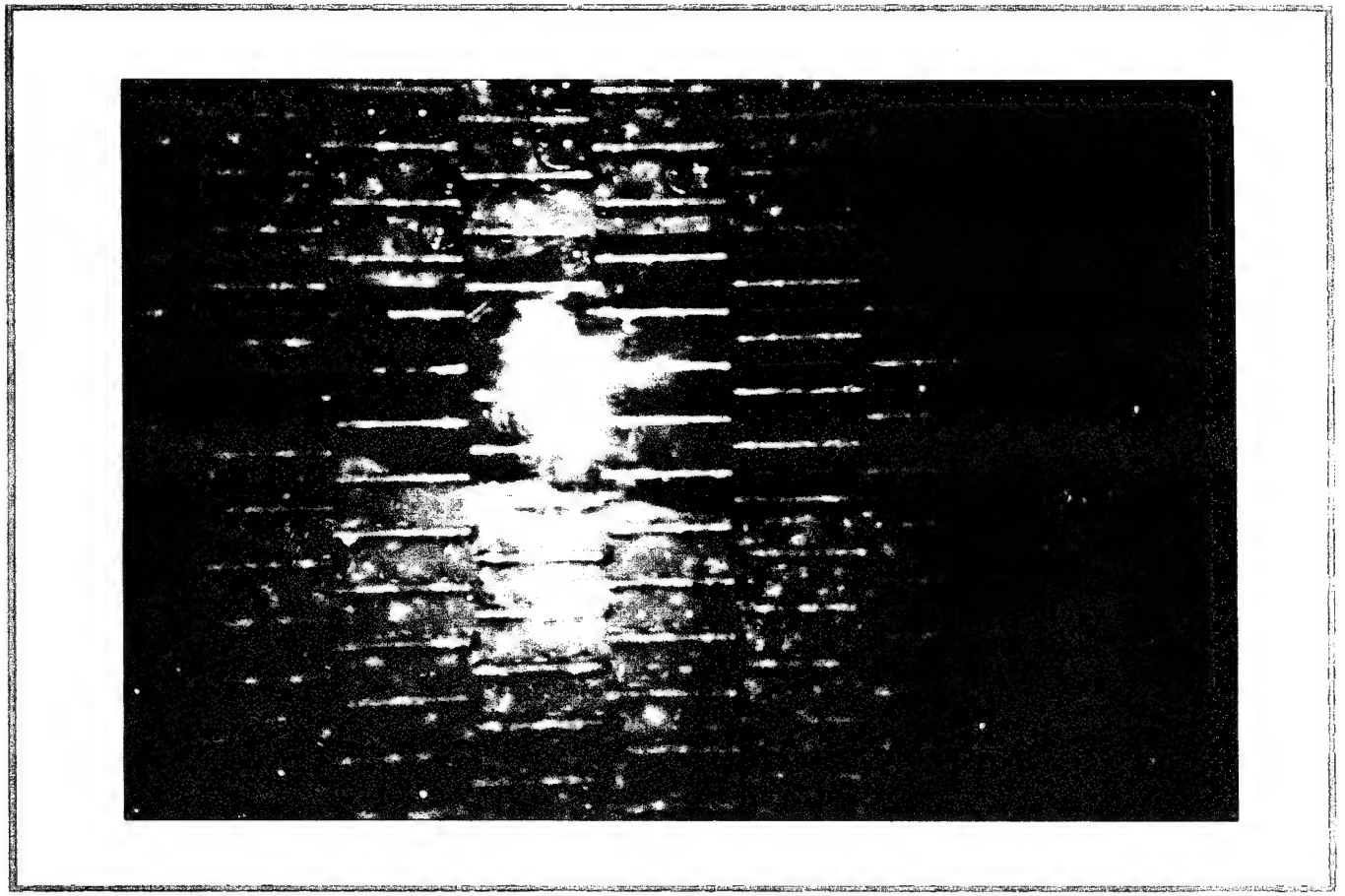

Figure 30. Flow Visualization of Water (Re = 200, After First Five Rows).

V. CONCLUSIONS

The heat transfer experiments of this study showed that, when the working fluid was water, the experimental values come to close agreement to the predicted values. But when Brayco Micronic 889 (PAO) was used as the working fluid, the experimental results were significantly higher than the predicted results. This provides evidence that the previous correlations were valid for water but not for PAO.

The comparison of the predicted dimensionless heat transfer coefficients to the experimental values validated the Prandtl number dependency of the Colburn j factor. It was obtained that the increase in the Colburn j factor was about the same with 1/3 to the power of the increase in the Prandtl number of the working fluid. This also proved the superiority of the higher Prandtl number fluids on the lower Prandtl number fluids to increase the performance of an heat exchanger.

Flow visualization experiments showed that, the interrupted geometry of the fins prevented the velocity boundary layers from getting excessively thick. Observing these laminar boundary layers along the offset strip fins helped to explain the enhancement in the heat transfer of the system for varying flow rates.

In general, this study will help the researchers to predict the dimensionless heat transfer coefficient of a ten times scaled up model of a liquid flow through module used in electronics cooling.

VI. RECOMMENDATIONS

In any continuation of this study the followings are recommended;

- Clean the water deposits on the base plate and offset strip fins and prepare the test section for the new study.

- Redesign and manufacture a stronger, pressure resistant plexiglas cover for the heat exchanger.

- Insert additional thermocouples into the inlet and outlet of the test section. Remove the heater and calibrate the thermocouples mounted on the bottom of the base plate fin assembly to a zero reference point.

- Repeat the experiments of the present study by using a pump with higher capacity to investigate the heat transfer and flow characteristics of the system for the turbulent flow.

- Develop a numerical solution to the flow through the offset strip fins and compare the solution with the experimental results.

- Investigate the Fanning friction factor and the effect of the fin thickness on the form drag.

APPENDIX A. FLOWMETER CALIBRATION

The flowmeter was calibrated in two different ways. The first one consisted of a comparison of the average voltage output to the average time to collect a specific volume of water as shown in Figure 31.

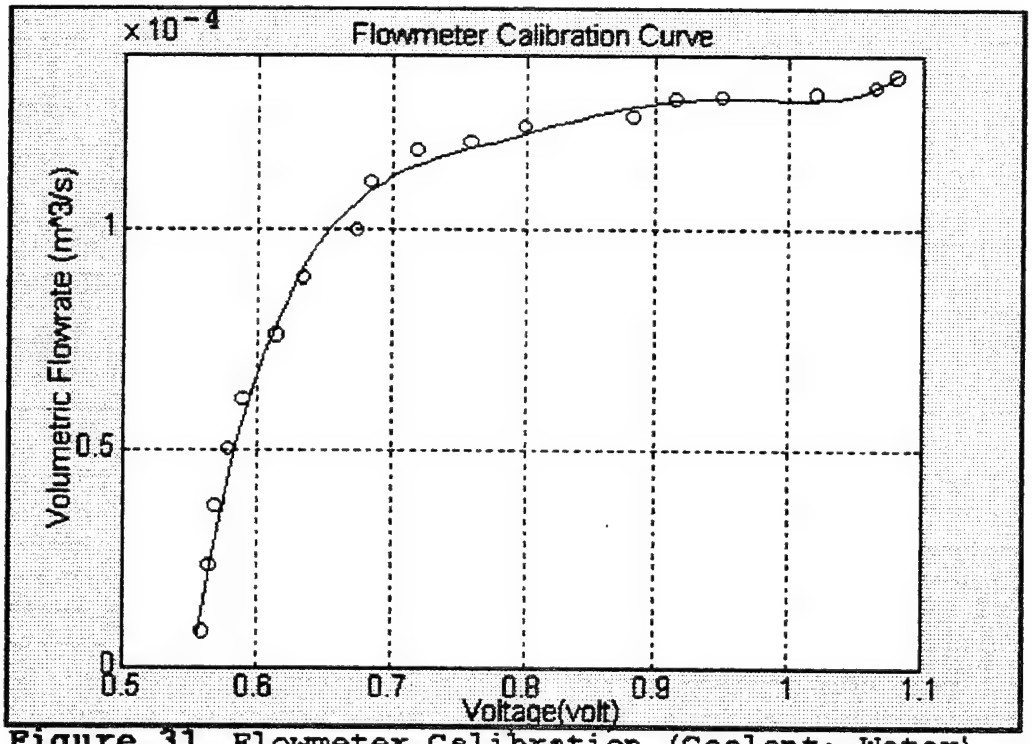

Figure 31. Flowmeter Calibration (Coolant: Water).

The second method was based on the collected mass of the water in a specific time for varying pump speeds as shown in Figure 32.

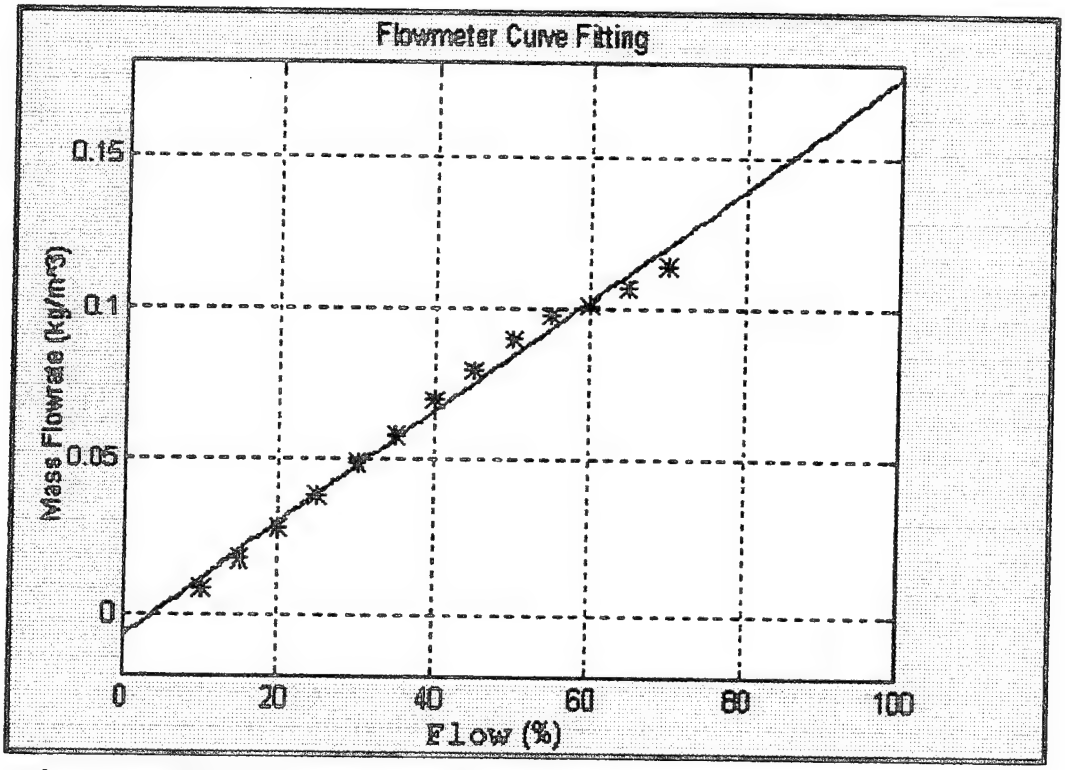

Figure 32. Flowmeter Calibration (Coolant: Water).

The calibration of the flowmeter for Brayco Micronic 889 Polyalphaolefin (PAO) was based on the first method which consisted the comparison of the flow percentage readings to the average time to collect a specific volume of PAO as shown in Figure 33.

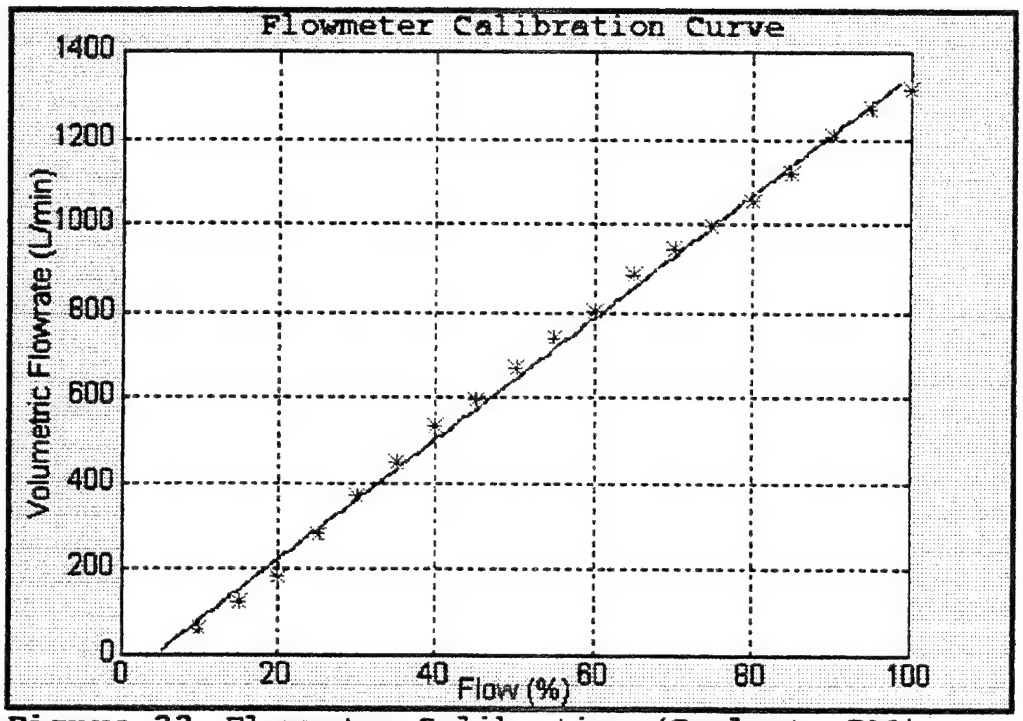

Figure 33. Flowmeter Calibration (Coolant: PAO).

APPENDIX B. QBASIC PROGRAM CODE

```
CLS
COLOR 14, 9
PRINT " Program for National Instruments PC2 IEEE-488 BOARD TO HP-3852"
PRINT " This uses the Universal Language Interface"
PRINT " ULI.COM must be run prior to running the program"
PRINT " The program name is  COLBURNJ.BAS"
PRINT " Modified by Ata KOMRAL"
OPEN "GPIB0" FOR OUTPUT AS #1
OPEN "GPIB0" FOR INPUT AS #2
PRINT #1, "ABORT"
PRINT #1, "RESET"
PRINT #1, "GPIBEOS CR LF"
PRINT #1, "CLEAR 9" STARTIT:
DIM TEMP(20), TMP(20), V(3), TIN(33), TOUT(33), DIFF(33), TAV(33), FILM(33),
TINSULA(33), TPGLSS(33)
PRINT #1, "REMOTE 9"
PRINT #1, "OUTPUT 9;RESET 700"
PRINT #1, "OUTPUT 9;USE 700"
INPUT "ENTER PUMP SETTING ", SET
TOTAV = 0!
TOTIN = 0!
TOTOUT = 0!
TOTDIFF = 0!
TOTFILM = 0!
TOTCVR = 0!
TOTINSL = 0!
N = 33
PRINT TIME$;
FOR J = 1 TO N
PRINT #1, "OUTPUT 9;CONF TEMPT "
FOR I = 0 TO 17
CHNL$ = STR$(I + 100)
MSG$ = "OUTPUT 9;MEAS TEMPT" + CHNL$
PRINT #1, MSG$
PRINT #1, "ENTER 9"
INPUT #2, TMP$
TMP(I) = VAL(TMP$)
NEXT I
PRINT #1, "OUTPUT 9; CONF TEMPT"
FOR I = 0 TO 17
```

```
CHN$ = STR$(I + 400)
MSGE$ = "OUTPUT 9; MEAS TEMPT" + CHN$
PRINT #1, MSGE$
PRINT #1, "ENTER 9"
INPUT #2, TEMP$
TEMP(I) = VAL(TEMP$)
NEXT I
PRINT #1, "OUTPUT 9;CONF DCV"
PRINT #1, "OUTPUT 9;USE 700"
FOR I = 0 TO 2
CH$ = STR$(I + 500)
MESS$ = "OUTPUT 9;MEAS DCV" + CH$
PRINT #1, MESS$
PRINT #1, "ENTER 9"
INPUT #2, VOLT$
V(I) = VAL(VOLT$)
NEXT I
PRINT #1, "CLEAR 9"
PRINT #1, "LOCAL 9"
TPLATE1 = 0!
I = 0
DO WHILE I < 12
I = I + 1
TPLATE1 = TPLATE1 + TMP(I - 1)
LOOP
TPLATE2 = 0!
I = 0
DO WHILE I < 11
I = I + 1
TPLATE2 = TPLATE2 + TEMP(I - 1)
LOOP
TSURF = (TPLATE1 + TPLATE2) / (12 + 11)
TIN = 0!
I = 0
DO WHILE I < 4
I = I + 1
TIN = TIN + TEMP(I + 11)
LOOP
INTMP = TIN / 4
TOUT = 0!
I = 0
DO WHILE I < 4
I = I + 1
```

```
TOUT = TOUT + TMP(I + 11)
LOOP
OUTTMP = TOUT / 4
TPGLASS = 0!
I = 0
DO WHILE I < 2
I = I + 1
TPGLASS = TPGLASS + TMP(I + 15)
LOOP
TCVR = TPGLASS / 2
TINS = 0!
I = 0
DO WHILE I < 2
I = I + 1
TINS = TINS + TEMP(I + 15)
LOOP
TINSUL = TINS / 2
TAV(J) = TSURF
TIN(J) = INTMP
TOUT(J) = OUTTMP
DIFF(J) = OUTTMP - INTMP
FILM(J) = (TSURF + INTMP) / 2
TPGLSS(J) = TCVR
TINSULA(J) = TINSUL
TOTAV = TOTAV + TAV(J)
TOTIN = TOTIN + TIN(J)
TOTOUT = TOTOUT + TOUT(J)
TOTDIFF = TOTDIFF + DIFF(J)
TOTFILM = TOTFILM + FILM(J)
TOTCVR = TOTCVR + TPGLSS(J)
TOTINSL = TOTINSL + TINSULA(J)
NEXT J
TSURFACE = TOTAV / N
INLET = TOTIN / N
OUTLET = TOTOUT / N
DELTA = TOTDIFF / N
FILMTEMP = TOTFILM / N
TCOVER = TOTCVR / N
TINSULATION = TOTINSL / N
DELTINSUL = TINSULATION - TCOVER
TEMDIF = TSURFACE - INLET
R = 2
P = V(2) * (V(1) / R)
```

```
FOR I = 0 TO 2
PRINT USING "###.##"; V(I);
NEXT I
PRINT "PWR="
PRINT USING "##.##"; P
FOR I = 0 TO 3
PRINT I + 100;
PRINT USING "###.###"; TMP(I);
PRINT I + 104;
PRINT USING "###.###"; TMP(I + 4);
PRINT I + 108;
PRINT USING "###.###"; TMP(I + 8);
PRINT I + 112;
PRINT USING "###.###"; TMP(I + 12)
NEXT I
FOR I = 0 TO 3
PRINT I + 400;
PRINT USING "###.###"; TEMP(I);
PRINT I + 404;
PRINT USING "###.###"; TEMP(I + 4);
PRINT I + 408;
PRINT USING "###.###"; TEMP(I + 8);
PRINT I + 412;
PRINT USING "###.###"; TEMP(I + 12)
NEXT I
PRINT #1, "OUTPUT 9;BEEP"
PRINT #1, "CLEAR 9"
PRINT #1, "LOCAL 9"
z = 19.5
l = .03175
s = .01175
t = .00152
h = .01524
Ah = .07742
Ac = s * h
Af = Ac * z
At = s * l + 2 * h * l + 2 * t * h
Dh = (4 * Ac) / (At / l)
vis = -(3.7292 / 10 ^ 12) * FILMTEMP ^ 3 + (7.125 / 10 ^ 10) * FILMTEMP ^ 2
- (5.0808 /        10 ^  8) * FILMTEMP + (1.7758 / 10 ^ 6)
kf = (8.3333 / 10 ^ 8) * FILMTEMP ^ 3 - (2.1429 / 10 ^ 5) * FILMTEMP ^ 2
+ (2.631 / 10 ^ 3) * FILMTEMP + .55206
Pr = (4.4271 / 10 ^ 7) * FILMTEMP ^ 4 - (1.0604 / 10 ^ 4) * FILMTEMP ^ 3
+ (9.9979 / 10 ^ 3) * FILMTEMP ^ 2 - (4.9008 / 10) * FILMTEMP + 13.6
```

```
den = (2 / 10 ^ 5) * FILMTEMP ^ 3 - (6.407 / 10 ^ 3) * FILMTEMP ^ 2
+ (3.207 / 10 ^ 2) * FILMTEMP + 1002.3
Cp = (5.2604 / 10 ^ 6) * FILMTEMP ^ 4 - (1.1167 / 10 ^ 3) * FILMTEMP ^ 3
+ (9.3021 / 10 ^ 2) * FILMTEMP ^ 2 - (3.2558) * FILMTEMP + 4217.8
m = .0018 * SET - .0073
Q = m / den
VEL = Q / Af
Re = (VEL * Dh) / vis
kins = .04
thick = .75 * 2.54 / 100
DELP = kins * Ah * DELTINSUL / thick
PTOT = P + DELP
FLUX = P / Ah
Nu = (FLUX * Dh) / kf / TEMDIF
Je = Nu / Re / (Pr ^ (1 / 3))
PRINT TIME$
PRINT "TAVG=";
PRINT USING "###.###"; TSURFACE;
PRINT "TIN=";
PRINT USING "###.###"; INLET;
PRINT "TOUT=";
PRINT USING "###.###"; OUTLET;
PRINT "DELTA=";
PRINT USING "###.###"; DELTA;
PRINT "TFILM=";
PRINT USING " ###.###"; FILMTEMP;
PRINT "TDIF=";
PRINT USING " ###.###"; TEMDIF;
PRINT "TCOVER=";
PRINT USING " ###.###"; TCOVER;
PRINT "TINSUL=";
PRINT USING " ###.###"; TINSULATION;
PRINT "visc=";
PRINT USING "###.######"; vis;
PRINT "cond=";
PRINT USING "##.######"; kf;
PRINT "Prandtl=";
PRINT USING "##.######"; Pr;
PRINT "Density=";
PRINT USING "####.#####"; den;
PRINT "Cp=";
PRINT USING "####.####"; Cp;
PRINT "POWER=";
```

```
PRINT USING "####.####"; PTOT;
PRINT "m=";
PRINT USING "###.####"; m;
PRINT "VEL=";
PRINT USING "###.#####"; VEL;
PRINT "Re=";
PRINT USING "###.#####"; Re;
PRINT "FLUX=";
PRINT USING "####.#####"; FLUX;
PRINT "Nu=";
PRINT USING "####.#####"; Nu;
PRINT "j=";
PRINT USING "####.#####"; Je;
INPUT "  DO YOU WISH TO SAVE DATA ?  ", SAVIT$
IF SAVIT$ = "n" THEN GOTO QUES
IF SAVIT$ = "N" THEN GOTO QUES
FILEIT:
PRINT " IF DATA FILE EXISTS OLD DATA WILL BE OVERWRITTEN "
INPUT "ENTER THE NAME OF THE DATA FILE TO CREATE", FILE$
IF FILE$ = "" THEN GOTO FILEIT
OPENIT:
OPEN FILE$ FOR OUTPUT AS #3
PRINT #3, DATE$
PRINT #3, TIME$
PRINT #3, "Pump Set =";
PRINT #3, SET
PRINT #3, "Elec.Power =";
PRINT #3, USING "###.###"; P
PRINT #3, "Act.Power =";
PRINT #3, USING "###.###"; PTOT
PRINT #3, "Lost =";
PRINT #3, USING "###.###"; DELP
PRINT #3, "Flowrate = ";
PRINT #3, USING "###.####"; m
PRINT #3, "Density = ";
PRINT #3, USING "###.####"; den
PRINT #3, "Viscosity = ";
PRINT #3, USING "###.####"; vis
PRINT #3, "Conductivity = ";
PRINT #3, USING "###.####"; kf
PRINT #3, "Prandtl = ";
PRINT #3, USING "###.####"; Pr
PRINT #3, "Cp = ";
```

```
PRINT #3, USING "###.####"; Cp
PRINT #3, "Velocity =";
PRINT #3, USING "###.####"; VEL
PRINT #3, "Reynolds =";
PRINT #3, USING "###.####"; Re
PRINT #3, "Flux =";
PRINT #3, USING "####.###"; FLUX
PRINT #3, " Nusselt =";
PRINT #3, USING "###.###"; Nu
PRINT #3, "Colburn j =";
PRINT #3, USING "###.####"; Je
PRINT #3, "Vflmtr =";
PRINT #3, V(0)
PRINT #3, "Vheat =";
PRINT #3, V(1)
PRINT #3, "Vresis =";
PRINT #3, V(2)
PRINT #3, "Thermocouples(C)"
FOR I = 0 TO 17
PRINT #3, (I + 100); TMP(I); (I + 400); TEMP(I)
NEXT I
PRINT #3, "Tsurf =";
PRINT #3, USING "###.##"; TSURF
PRINT #3, "Tfilm =";
PRINT #3, USING "##.###"; FILMTEMP
PRINT #3, "Tin =";
PRINT #3, USING "##.###"; INLET
PRINT #3, "Tout =";
PRINT #3, USING "##.###"; OUTLET
PRINT #3, "Delta = ";
PRINT #3, USING "##.###"; DELTA
PRINT #3, "Tdiff = ";
PRINT #3, USING "##.###"; TEMDIF
PRINT #3, "Tcover = ";
PRINT #3, USING "##.###"; TCOVER
PRINT #3, "Tinsulation = ";
PRINT #3, USING "##.###"; TINSULATION
QUES:
INPUT " DO YOU WISH TO TRY ANOTHER RUN ( Y/N ) ? ", AGAIN$
IF AGAIN$ = "Y" THEN GOTO STARTIT
IF AGAIN$ = "y" THEN GOTO STARTIT
IF AGAIN$ = "N" THEN END
IF AGAIN$ = "n" THEN END
GOTO QUES
END
```

APPENDIX C. PROPERTIES OF BRAYCO MICRONIC 889 (PAO)

The properties of Brayco Micronic 889 Polyalphaolefin taken from Ref. 10 are tabulated below. The thermal conductivity of Brayco Micronic 889 (PAO) was 0.083-0.085 $BTU/hr.ft^2$ during the heat transfer experiments.

TEST (ASTM)	DESCRIPTION	RESULT
D-445	Kinematic Viscosity	(10^6 m^2/s)
	@ 100 °C	1.7
	@ 40 °C	52
	@ -40 °C	260
	@ -54 °C	1200
D-287	Density	(g/ml)
	@ 0 °C	0.811
	@ 20 °C	0.794
	@ 40 °C	0.777
	@ 100 °C	0.723
	@ 160 °C	0.661
D-2766	Specific Heat	(cal/g C)
	@ -18 °C	0.49
	@ 10 °C	0.52
	@ 38 °C	0.54
	@ 93 °C	0.58

Table 9. Properties of Brayco Micronic 889[Ref. 10].

APPENDIX D. SAMPLE CALCULATIONS

The following calculation is for the following setpoint.

Coolant : Water.

Electrical Power Input , P_{Elc}= 100.172 Watts.

Flow (%) = 40.

Mass Flow Rate, m = 0.0647 kg/s.

Inlet Temperature, T1 = 20.05 °C

Outlet Temperature, T2 = 20.26 °C

Plate Average Temperature, T3 = 24.02 °C

Temperature Difference Through the Insulation Layer, ΔT_{insul} = 3.088 °C

1. Characteristic Dimension

$$A_c = s \times h$$
$$A_c = 11.75mm \times 15.24mm.$$
$$A_c = 179.1mm^2.$$

$$A_f = M \times A_c$$
$$A_f = 19.5 \times 179.1$$
$$A_f = 3492.5mm^2.$$

$$A = s \times l + 2 \times h \times l + 2 \times h \times t$$
$$A = (11.75 \times 31.75) + (2 \times 15.24 \times 31.75) + (2 \times 15.24 \times 1.52)$$
$$A = 1387.1mm^2.$$

$$D_h = \frac{4A_c}{(A/l)} = \frac{4 \times 179.1}{(1387.1/31.75)} = 16.39mm.$$

2. Properties of Water

Film Temperature, $T_f = \frac{T1+T3}{2} = \frac{20.05+24.02}{2} = 22.04$ °C

Using Table A.6 [Ref. 9];

$\rho = 1000.11$ kg/m^3

$k_f = 0.6005$ W/m.K

Pr = 6.625

$C_p = 4180.51$ J/kg.K

$\mu = 9.623 \times 10^{-4}$ N.s/m^2

3. **Reynolds Number**

Volumetric Flow Rate, $Q = \frac{m}{\rho} = \frac{0.0647}{1000.11} = 6.469 \times 10^{-5}$ m^3/s.

Velocity, $V = \frac{Q}{A_f} = \frac{6.469 \times 10^{-5}}{3492.5 \times 10^{-6}} = 0.0185$ m/s.

$$Re_D = \frac{\rho \times V \times D_h}{\mu} = \frac{(1000.11) \times (0.0185) \times (16.39 \times 10^{-3})}{9.623 \times 10^{-4}} = 315.65$$

4. **Nusselt Number**

Lost/Gained Heat, $\Delta P = \frac{-k_{insul} \times A_h \times \Delta T_{insul}}{t_{insul}}$

where k_{insul} (0.04 W/m.K), is the thermal conductivity and t_{insul} (0.01905), is the thickness of the insulation layer.

$$\Delta P = \frac{-(0.04) \times (0.07742) \times (3.088)}{0.01905} = -0.502 \text{ Watts.}$$

Total Power Input, $P = P_{Elc} - \Delta P$

$$P = 100.172 + 0.502 = 100.674 \text{ Watts.}$$

Heat Flux, $q'' = \frac{P}{A_h} = \frac{100.674}{0.07742} = 1300.36$ W/m^2.

$$Nu_{avg} = \frac{q'' \times D_h}{k_f \times (T3 - T1)} = \frac{(1300.36) \times (16.39 \times 10^{-3})}{(0.6005) \times (3.97)} = 8.94$$

5. **Colburn j Factor**

$$j = \frac{Nu_{avg}}{Re_D \times \mathrm{Pr}^{1/3}} = \frac{8.94}{(315.65) \times (6.625)^{1/3}} = 0.0151$$

APPENDIX E. UNCERTAINTY ANALYSIS

The accuracy of the results of this study was estimated by performing an uncertainty analysis. The theorem established by S .J. Kline and F. A. McClintock [Ref. 11] was used to calculate the uncertainties. In this theorem a calculated result y is a function of several independent measured variables, $\{x_1, x_2, \ldots\ldots, x_n\}$. Each measured value has some uncertainty, $\{u_1, u_2, \ldots\ldots, u_n\}$, and these uncertainties lead to an uncertainty in y, which is called u_y. To estimate u_y, it's assumed that each uncertainty is small enough that a first-order Taylor expansion of $y(x_1, x_2, \ldots\ldots x_n)$ provides a reasonable approximation. Under this approximation, y is a linear function of the independent variables and the uncertainty is determined by :

$$u_y = \left[\left(\frac{\delta y}{\delta x_1} u_1 \right)^2 + \left(\frac{\delta y}{\delta x_2} u_2 \right)^2 + \cdots + \left(\frac{\delta y_n}{\delta x_n} u_n \right)^2 \right]^{1/2}$$

Here, all uncertainties must have the same odds and must be independent of each other. For $y = A\frac{x_1^m x_2^n}{x_3^k}$, the uncertainty takes the following form;

$$\frac{u_y}{y} = \left[\left(m\frac{u_1}{x_1} \right)^2 + \left(n\frac{u_2}{x_2} \right)^2 + \left(k\frac{u_3}{x_3} \right)^2 \right]^{1/2}$$

The uncertainty analysis performed for the power setting of **100** Watts and the Reynolds number of about **315.65** (for water) which produced a Colburn j factor of **0.0151** is presented below:

1. Reynolds Number Uncertainty

$$\mathrm{Re} = \frac{\rho \times D_h \times V}{\mu}$$

where $\frac{\delta Re}{Re} = \left[\left(\frac{\delta V}{V} \right)^2 + \left(\frac{\delta D_h}{D_h} \right)^2 \right]^{1/2}$ and $\frac{\delta D_h}{Dh} = \left[\left(\frac{\delta A_c}{A_c} \right)^2 + \left(\frac{\delta\left(\frac{A}{l}\right)}{\frac{A}{l}} \right)^2 \right]^{1/2}$

For $T_{film} = 22.04°C$

$\rho = 1000.11\ kg/m^3$, $k = 0.6005\ W/m.K$, $\mu = 9.62\ E\text{-}4\ N\text{-}s/m^2$, $Pr = 6.625$

$A_c = 0.0001791\ m^2$. $\delta A_c = 0.00000962\ m.$

$A/l = 0.0437\ m.$ $\delta(A/l) = 0.000707\ m.$

$D_h = 0.01639\ m.$ $\delta D_h = 0.000919\ m.$

$V = 0.0185\ m/s.$ $\delta V = 0.0005\ m/s$

The uncertainty $\delta Re/Re = 0.0622$ (6.22 %) or $Re = 315.65 \pm 19.63$

2. Colburn j Factor Uncertainty

$$j = \frac{Nu_{avg}}{Re.\,Pr^{1/3}}$$

and

$$\frac{\delta j}{j} =$$

where,

$$\frac{\delta Nu}{Nu} =$$

For $q" = 1300.36\ W/m^2$. $\delta q" = 43.32\ W/m^2$.

$\nabla T(T3 - T1) = 3.97\ °C$. $\delta \nabla T = 0.1\ °C$.

$Nu_{avg} = 8.94$ $\delta Nu_{avg} = 0.625$

$j = 0.0151$ $\delta j = 0.0014$

The uncertainty $\delta j/j = 0.093$ or 9.3 %

LIST OF REFERENCES

1. WING AUNG, "Cooling Technology for Electronic Equipment", 1988.

2. T.Y. TOM LEE, JAMES A. ANDREWS, PETER CHOW and DAVID SAUMS, "Compact Liquid Cooling System for Small Movable Electronic Equipment", IEEE Transections or Components, Hybrids and Manifacturing Technology, Vol.15, No.5 October 1992.

3. WEITING, A.R., "Emprical Correlations for Heat Transfer and Flow Friction Characteristics of Rectangular Offset Fin Plate Heat Exchangers", Trans. ASME, Journal of Heat Transfer, Vol. 97, Series C, 488-490, 1975.

4. MANGLIK, R.M. and BERGLES, A.E, "The Thermal Hydraulic Design of the Rectangular Offset Strip Fin Compact Heat Exchanger", Compact Heat Exchangers, Hemisphere, 123-140, 1940.

5. WEBB, R., "Advances in Modeling Enhanced Heat Transfer Surfaces", Heat Transfer 1994 Proceedings of the Tenth International Heat Transfer Conference, Vol.1, G.F. HEWITT, Ed., Taylor Francis, Bristol, Pa., 1994.

6. KAYS, W.M., "Compact Heat Exchangers" in AGARD Heat Exchangers, AGARD-LS-57, Advisory Group for Aerospace Research and Development, NATO, Paris 1972.

7. S.V. PATANKAR and C. PRAKASH, "An Analysis of the Effect of Plate Thickness on Laminar Flow and Heat Transfer in Interrupted-Plate Passages", Int. J. Heat Mass Transfer, Vol.24, 1801-1810, 1981.

8. LT. JEFFREY M. MASTERSON, "Heat Transfer Studies on a Rectangular Channel With an Offset Plate Fin Array", Thesis, December 1993.

9. F. P. INCROPERA, D.P. DEWITT, "Introduction To Heat Transfer", Second Edition, Table A-6., A22-A23, 1990.

10. CASTROL, Speciality Products Division, "Brayco Micronic 889 Product Data Sheet", Irvine, CA, September 1994.

11. KLINE, S. J., and F. A. McClintock, Describing Uncertainties in Single-Sample Experiments. Mech. Engr. 75: 3-8, January 1953.

INITIAL DISTRIBUTION LIST

1 Defense Technical Information Center 2
Cameron Station
Alexandria, Virginia 22304-6145

2 Library, Code 52 2
Naval Postgraduate School
Monterey, California 93943-5101

3 Professor M.D. Kelleher 3
Department Chairman, Code ME
Naval Postgraduate School
Monterey, California 93943-5000

4 Naval Engineering Curricular Officer, Code 34 1
Department of Mechanical Engineering
Naval Postgraduate School
Monterey, California 93943-5000

5 Mr. Tony Buechler 1
Naval Weapons Support Center
Code 6042
Crane, Indiana 47522

6 Ms. Jennifer Campbell 1
471 36th Ave.
San Francisco, California 94121

7 Deniz Kuvvetleri Komutanligi 4
Personel ve Egitim Daire Baskanligi
Bakanliklar / ANKARA - Turkey

8 Istanbul Teknik Universitesi 1
Makina Muhendisligi Fakultesi
Isi Transferi Kursusu
Ayazaga / ISTANBUL - Turkey

9 Bogazici Universitesi 1
Makina Muhendisligi Fakultesi
Isi Transferi Kursusu
ISTANBUL - Turkey

10 Ortadogu Teknik Universitesi 1
Makina Muhendisligi Fakultesi
Isi Transferi Kursusu
ANKARA - Turkey

11 Mr. Fevzi Komral 1
Gencosman Mah. Guzeller Sok.
Ozen Sitesi B-Blok No: 4
Gungoren ISTANBUL - Turkey

12 Ltjg. Ata Komral 1
Gencosman Mah. Davutpasa Cad.
Gecit Sok. No: 8
Gungoren ISTANBUL - Turkey